RESPONSE TO THE REVIEWS:

Anonymous Referee #1

Response to Referee #1

(Line numbers refer to the new version of the article.)

General Comments:

Although this is a very important aspect as they correctly present it, the main topic Fe (II)/Fe (III) availability is not well described. In some aspect they are too brief such that their final results cannot be appreciated. However, it is an important topic that meets the requirements of publication at ACP. I would recommend that major revisions are done prior to consideration of a possible publication.

1. There is not enough evidence that the high soluble content they observe is due to Saharan dust. They need to show some correlations which lead to such arguments.

R: Yes, we agree with the reviewer's comment. The text was adjusted to show the correlations of the soluble contents with physical and chemical properties of long-range transported aerosol plumes. We are confident that the manuscript in its revised version convincingly shows that indeed a pronounced Saharan dust plume has been collected, which is the only plausible explanation for the increased Fe concentrations. Our argumentation is further supported by a broad set of related literature that is consistent with our observations. In general, this experiment was designed to obtain soluble iron measurements in aerosols originating from Saharan dust plumes. To achieve this goal, the following strategies were adopted:

Location - the progress of African dust occurrences across the Amazon can be readily followed by satellite images, which typically show that it takes about 1 week for dust outbreaks to cross to the Atlantic (Yu et al., 2015). The sampling site is located in the common transport pathway of Saharan dust and receives dust laden air masses on seasonal cycles.

Period of the year - several papers have shown that Saharan dust reaches the Amazon Basin especially during the months of March/April/May: (L.106-108) "The sampling period ranged from 19 March to 25 April

2015, which is within the typical season when dust transport to the Amazon Basin has been reported before (Talbot et al., 1990; Swap et al., 1992; Prospero et al., 2014; Yu et al., 2015)"

Iron source - studies have shown that in Central Amazonia, the iron content in aerosols originates from crustal sources or long range transport: (L. 342-344): "Soil dust related elements are typically present at the highest concentrations during the early wet-to-dry season transition (May), as has been shown in previous studies (Pauliquevis et al., 2012; Andreae et al., 2015)" (L. 358-361): "Pauliquevis et al. (2012) also observed increases in the concentration of total Fe with values reaching 60 ng m^{-3} in the fine mode mostly during February to April in the Amazon Basin, with a seasonal average of 36 ng m^{-3}. They attributed this to episodes of Saharan dust transport."

2. Simply because the air mass originates from Africa does not imply all chemical components in the aerosol are from the Saharan Desert. This aspect has to be clarified and the identification of the sources that could lead to different soluble iron concentrations in this region has to be discussed.

R: We agree with the reviewer. The long-range transported aerosol from Africa typically comprises a complex mixture of desert dust, biomass burning smoke, maritime aerosols, and biological particles. The revised discussion on the elements measured in the aerosol samples and their potential origin from the aforementioned sources has been extended. We show that the dust fraction is the only plausible explanation for most of the Fe content, whereas Na, Cl, Mg, K, and other elements are associated with sea spray and biomass burning aerosol fractions in the long-range transport plumes.

Specifically, we are referring to the Sahara and Sahel region together as "Sahara". This has been stated in the abstract. In addition to mineral dust aerosol from the Sahara and/or Sahel region, there is also marine aerosol introduced from the Atlantic Ocean, which can contribute sea salt elements and biogenic sulfate.

Because the northern hemisphere winter is also the fire season in West Africa, biomass burning smoke often arrives together with African dust. This can be seen in the BCe concentration of up to 0.3 µg m^{-3} on 4 April. At a typical fraction of 7% of BC in biomass TPM, this could contribute about 4 µg m^{-3} of TPM, or about 20% of the TPM at the peak of the BCe concentration. We have added a comment on this in the text.

But regarding our main goal, Longo et al. (2016) indicated that the iron in Saharan dust exhibits different oxidation states across the different sampling sites, suggesting that the longer an aerosol remains in the atmosphere, the more reduced the iron becomes. These complex interactions suggest that the various particle-aging mechanisms, such as acidic reactions and photoreduction, may be working simultaneously.

(L. 220-224) Although the Hysplit backward trajectories do not guarantee that pure end members were sampled, they help to demonstrate that most air masses were of North African origin during the sampling time periods.
(L. 351-356) The concentration of iron (II) obtained recently at Barbados is in the same order of magnitude as the amounts that we measured (Zhu et al., 1997). Additionally, the increase in particle number measured during the sampling period correlated with the presence of Saharan aerosols at the ATTO site.

3. There should be more clarity on the experimental approach on how they measured the soluble metals.

R: We agree with the reviewer. The experimental details in section 2.2 have been specified in more detail (L.128-146) "All the analyses were performed on the TPM soluble fraction. Each sampled filter immersed in nitric acid solution was extracted by an ultrasonic bath for 10 mins. The extract of each sample was filtered with a polyvinylidene difluoride (PVDF) sterile membrane (0.22 µm pore size, diameter 25 mm, Millipore, Merck) and analysed by ion chromatography (ICS 5000, Dionex-Thermo Scientific, USA).
For the transition metal quantification and iron speciation, pyridine-2,6-dicarboxylic acid (PDCA) was used as eluent and 4-2-2-pyridyl resorcinol (PAR) was used as a post-column reagent, stabilized by a PC-10 nitrogen pump. The system flow was 0.3 mL min^{-1} through an IonPac CG5A (2 x 50 mm) guard column, CS5A capillary column (2 x 250 mm) and UV-Vis spectrophotometry with detection at 530 nm (Cardellicchio et al., 1997). For soluble Fe (II), Fe (III), Cu and Zn the detection limits (USEPA, 1997) were 1.7, 0.4, 1.3, 4.1 µg L^{-1}, respectively and the expanded uncertainties at the 95% level of confidence (BIPM, 2008) were of 3, 42, 46, 56 %, respectively.
For the cation analysis, ultrapure water and methanesulfonic acid (MSA) was used as the eluent at a 20 mM constant concentration, with automatic suppression (CSRS suppressor - 2 mm), and with a 0.33 mL min^{-1} system flow through an IonPac CG-12 guard column (2 x 50 mm) and CS-12 (2 x 250 mm) capillary column. This resulted in a 14 min running time for each injection. For soluble Na, NH_4^+, K, Mg and Ca the detection limits (USEPA, 1997) were 2.0, 1.3, 0.9, 0.7, 1.8 µg L^{-1}, respectively, and the expanded uncertainties at the 95% level of confidence (BIPM, 2008) were of 9, 7, 21, 11, 23 %, respectively."

Specific Comments:

4. How long did the samples stay in the nitric acid flask and were they any measurements done to ensure

that the transition from Fe (II) to Fe (III) or vice versa did not occur during the time frame of storage?

R: The samples stayed in the nitric acid flask during the sampling period of March 19th to April 25th and no test was performed during the storage period. Based on Cwiertny et al (2008), the dissolved Fe(II) / Total dissolved Fe ratio of Saharan Dust, is practically constant over time: "Nitric acid suppresses the formation of iron(II) at low pH; therefore, pH can also act as a control of oxidation state of aerosol iron."

5. Where the extracts filtered? The experimental part is too brief to follow the obtained results.

R: The method section was rewritten with more details and the required information was added to the text as follows: (L. 128-132) "Each sampled filter immersed in nitric acid solution was extracted by an ultrasonic bath for 10 mins. The extract of each sample was filtered through a polyvinylidene difluoride (PVDF) sterile membrane, 0.22 µm pore size, diameter 25 mm (Millipore, Merck) and analysed by ion chromatography (ICS 5000, Dionex-Thermo Scientific, USA)."

6. What were the concentrations of the total fractions of each of the elements?

R: The focus of the sampling efforts was to quantify the soluble fraction. In order to keep the oxidation state of iron stable, we immersed the filters in the acidic solution. The chemical analysis performed was Ion Chromatography and to assess the total fraction we used TPM elemental composition results sampled simultaneously at another site, as detailed in Table 1 (L.788-790). Previous studies have shown that the aerosol composition and burden is almost identical at the two sites when long-range transport is dominant, as it was during our study.

7. How could the fungi be optimally identified using a light microscope? Was there an algorithm that matched the shapes of the fungi to given types of fungi in a library or was it simply done by intuition?

R: The fungi types were identified using consolidated data bases and a certified spore counter with the US National Allergy Bureau: (L. 2143-214).

8. How good could the mineral dust adsorption in the black carbon signal be isolated since it's mentioned

that mineral dust could also produce similar adsorption signals?

R: The absorption Angstrom exponent (AAE) can be used to investigate the relative contribution of different particle sources to the BCe signal. Particle samples impacted by mineral dust typically show AAE greater than 2.0, while soot from fossil fuel combustion shows AEE close to 1.0 (e.g., Bergstrom et al., 2007). There are methods proposed in the literature to distinguish between fossil fuel soot and other light absorbing particles (e.g., Lack and Langridge, 2013), but we consider that this is not in the scope of the present article. However, to clarify this point, we reformulated part of sections 2.4 and 3.1 as follows:

(L. 164-174): "Soot, mineral dust, and biogenic particles are light absorbers (Moosmüller et al., 2009; 2011; Guyon et al., 2004; Andreae and Gelencsér 2006) and may contribute to the observed BCe signal. The relative contributions of particle sources to BCe can be investigated by considering the absorption spectral variability, by means of the so called Absorption Ångström Exponent (AAE). Soot from fossil fuel combustion typically shows AAE close to 1.0, while particles impacted by dust emissions show AAE greater than 2 (Bergstrom et al., 2007). Studies indicate that samples impacted by biomass burning aerosols show AAE in the range of 1.5-2.0 (Bergstrom et al., 2007; Rizzo et al., 2011). The spectral dependency of particle absorption coefficients was monitored using a 7-wavelength Aethalometer (Model AE33, Magee Scientific Company, USA, λ = 370, 470, 520, 590, 660, 880, and 950 nm), compensated for filter loading and multiple scattering effects (Rizzo et al., 2011)."

(L. 236-252): "Particulate Fe(III) and Fe(II) concentrations increased between 3 and 9 April, simultaneously with an increase in particle absorption and scattering coefficients (Figure 4.a). A decrease was observed in the intrinsic property, single scattering albedo (SSA, Figure 4.b), suggesting the presence of particles that are efficient light absorbers, such as soot from fossil fuel combustion and biomass burning, mineral dust, and biogenic particles. For comparison, Rizzo et al. (2013) reported that a 7% decrease in SSA at another forest site in the central Amazon during the wet season periods proved to be related to advection of African aerosols. The spectral dependency of absorption, AAE, can be used to distinguish between the different sources of light absorbing particles. The elevated AAE values observed between 6 and 10 April (Figure 4.b) contradict the influence of soot from fossil fuel combustion. During the clean periods (25 March to 2 April and 16 to 24 April), dominated by biogenic particles, AAE values were around 1.8, so that this source of particles, ever present at Amazonian forest sites, may not have contributed to the AAE increase between 6 and 10 April.

Therefore, two light absorbing particle sources are left to explain the increase in absorption and AAE values: biomass burning and mineral dust particles. Fire activity is typically low in the central Amazon between November and April, with less than 2 fire spots per 1000 km2 and day on average (Castro-Videla et al., 2013),

which is corroborated by the map of fire spots distribution during the campaign period (Figure 5)."

(L. 280-283): "Our conclusion that African dust dominates the aerosol budget during the dust event is in agreement with Castro Videla et al. (2013), who, based on a five-year study, concluded that peaks in AOD in the central Amazon during the wet season had a significant contribution from coarse mode particles, pointing to a major role of African advection."

9. The soluble Fe concentration seems to be high for pure Saharan dust. It is known that in lower pH the solubility can be as high as 10% or more. However, it would be helpful to explain in detail how the samples were prepared.

R: Yes, we agree with the reviewer and the methods section was modified: (L. 128-146). Regarding the required information, each sampled filter immersed in nitric acid solution was extracted by ultrasonic bath. The extract of each sample was filtered through a PVDF sterile membrane, 0.22 µm pore size, diameter of 25 mm and analyzed by ion chromatography for Na^+, NH_4^+, K^+, Mg^{2+}, Ca^{2+}, Fe^{3+}, Cu^{2+}, Zn^{2+} *and* Fe^{2+}.

10. How did you differentiate the sources of the soluble Fe? As mention in the literature comparisons, Fe has other sources, such as combustion, industrial emissions. Iron from these sources in some cases has been found to be more soluble than in Saharan dust. It is unclear from your arguments, why you allocate the soluble iron to be originating from Saharan dust. Long range transport is a mixture of different air masses and these air masses may have different chemical compositions. Thus a more detailed tracer analysis or correlation of an intrinsic dust element such as Al or Ti would be helpful to identify how significant the Saharan dust contributed to the obtained soluble iron concentrations.

R: The reviewer is correct. It is very hard to determine sources based on trajectories/long transport alone. The ATTO site, especially its location, was chosen to provide the most reliable sampling of natural tropical aerosols in the world. It is in one of most remote areas on the planet, and this is the primary reason why we assert that our aerosol samples were mostly from natural contributions. As explained in the answer to the first question, air masses reaching the site have crossed more than 1500 km of primary rainforests in the Amazon Basin. The bulk of the background aerosol at ATTO is biogenic. There are no industries in the path of these air masses.

(L. 267-277): "Biomass burning in Africa could also have contributed some of the observed Fe, but unfortunately, little is known about Fe emissions from savanna fires, and the available data span a wide range.

From the work of Gaudichet et al. (1995), one can derive a Fe content of 0.016% in savanna smoke TPM, which, at a peak biomass smoke concentration of 4 μg m−3, would only give 0.6 ng Fe m−3. Using the BC/Fe ratio of ca. 40 from Maenhaut et al. (1996) and the peak BCe concentration of 0.3 μg m−3, we can estimate ca. 8 ng Fe m−3. Finally, using the Fe emission factor of 0.026 g kg−1 d.m. for African savanna fires from Andreae et al. (1998) and the BC emission factor of 0.6 g kg−1 from Andreae and Merlet (2001 and updates), we can estimate a peak pyrogenic Fe contribution of 13 ng m-3. This compares to 64 ng m −3 of soluble iron (details follow in section 3.3) at the same time, and, given that only a small fraction of the Fe in biomass smoke is likely to be soluble, it is clear that the dominant fraction of soluble Fe comes from the African mineral dust."

We are quite confident of our results because when we compare with dust obtained at Barbados, we observed that the soluble ferrous iron (Fe(II)) and Total soluble iron (Fe) are in the same order of magnitude (Zhu et al., 1997).

11. What could be the likely reason for the high wind and high Fe (III) correlation observed above the canopy?

R: These vertical transport correlations could be analyzed by micrometeorological methods (e.g., eddy covariance). However, this analysis is beyond the scope of this work. The idea of presenting the vertical speed was only to show that regardless of the cloudy conditions, the W values are close to zero, indicating that the vertical transport is very weak. Thus, the text was rewritten to make this clear. The vertical wind data have been removed.

12. How good did the soluble content correlate with the BC content and total mass concentration?

R: We thank the reviewer for this opportune suggestion, and added the time series of BCe and particle soluble fraction concentration to Figure 2. This clearly shows that the latter are well correlated with total mass concentration, especially during the event from April 1 to 8. We also added the following sentence to the section 3.2: (L. 315-318) "Figure 2 and Table 1 show that BCe concentrations significantly increased regionally during 1-8 April, coinciding with the increase in PM10 and particle soluble fraction concentrations and indicating that some biomass smoke (probably from fires in West Africa) arrived together with the dust".

Anonymous Referee #2

Response to Referee #2

Abstract

1. The problem of this manuscript that begins by the Title and the Abstract is the generalization of ideas. First I suggest that the authors be more specific in the Title, it should focus on the soluble fraction Fe(II)/Fe(III) issue, which is something important but not enough to account a full story about the Amazon rainforest ecology.

R: Yes, we agree with the reviewer, and the title was changed to: "Soluble iron nutrients in Saharan dust over the central Amazon rainforest" to match better with the main goal. The text was also restructured to emphasize the iron soluble fraction and the frequent long-range transport of African aerosols.

2. In the introduction, clarify at Line 124 (pag 6) when the authors say ": Considering that iron is absorbed by plants only as soluble Fe(II)/Fe(III)", previously the authors have stated that Fe(III) was also recovered by the action of rhizosphere.

R: The sentence was confusing as indicated by the reviewer. Plants require the micronutrient iron in small amounts and the absorption can vary according to the species. Iron uptake can be as Fe (II) or (III) and the absorption fraction depends on the ability of the plant to reduce it to Fe (II). In this role, the pH is important for solubility and therefore the iron availability. The text has been changed accordingly.

3. In methods, Line 142, pag 6, provide filter porosity.

R: The information was added to the text as follows: (L. 111-112)"Atmospheric particles were collected on Nuclepore® polycarbonate filters (47 mm diameter, 0.8 μm pore size, Whatman® Nuclepore)"

4. In Item 2.5, specify how the samples were storage and if the observations were conducted in the filed or in a particular laboratory condition?

R: After sampling the filters were stored at 4°C in the field and then carried to a laboratory to perform the ion

chromatography analysis. The information was added to the text: (L. 117-118) "After sampling, the filters were immediately stored in sterile flasks under refrigeration until laboratory analysis."

5. The sentence in Line 229-231 "The mass concentration of particles over the Amazon Basin in the wet season is typically around 10 ug m-3 in locations that are influenced by biomass burning emissions", : : : here there is confusion on the wet season and biomass burning season. Which reference is attributed to the mass concentration mentioned?

R: The reviewer is right, the information was confusing. The text was rewritten as follows: (L. 291-297)" The mass concentration of PM10 particles in Amazonia is close to background in most areas throughout the basin during the wet season. Central Amazonia is characterized by a weak influence of anthropogenic emissions and aerosol mass concentrations are low during the wet season - typically 7 μg m−3; even the most impacted areas do not exceed 10 μg m−3 due to intensive rain and the corresponding inhibition of biomass burning (Artaxo et al., 2002; Artaxo et al. 2013; Martin et al., 2010). Increased mass concentrations may occur due to African dust events that reach the Amazon forest in this season (Talbot et al., 1990; Martin et al., 2010)."

6. Part of the text in Lines 254 to 268 (pags 11-12) could be placed at Material and Methods. If possible the authors could place BCe time series superimposed to mass concentrations at Figure 1. This could give some idea on the contribution of BC to the bulk atmospheric concentrations, or if they are lagged in time.

R: Following the referee's suggestion, we moved part of the text from the Results to the Material and Methods section. Part of section 2.4 was reformulated as follows:

(L. 160-168) "Equivalent black carbon concentrations (BCe) were obtained by a Multi Angle Absorption Photometer (MAAP, Model 5012, Thermo Electron Group, USA; λ = 670 nm), based on light absorption measurements at 637 nm. An absorption cross section value of 6.6 m2 g was used for the conversion of measured absorption coefficients into BCe concentrations (Petzold et al., 2005). Soot, mineral dust, and biogenic particles are light absorbers (Moosmüller et al., 2009; 2011; Guyon et al., 2004; Andreae and Gelencsér 2006) and may contribute to the observed BCe signal. The relative contributions of particle sources to BCe can be investigated by considering the absorption spectral variability, by means of the so called Absorption Ångström Exponent (AAE)."

The information was also added in section 3.2:

(L. 310-311) "The concentrations of black carbon equivalent (BCe) measured online during this intensive campaign represented on average 1.5% of PM10 mass concentrations, ranging from 0 to 0.3 µg m−³." (L. 315-317) "Figure 2 and Table 1 show that BCe concentrations significantly increased regionally during 1-8 April, coinciding with the increase in PM10 and particle soluble fraction concentrations"

7. In Table 2, how the elemental analysis was conducted for Cu, Zn, Na, Ca, K and Mg? and about the NH4 ?

R: The experimental details were included in the Methods section as follows:(L. 140-146) "For the cation analysis, ultrapure water and methanesulfonic acid (MSA) was used as the eluent at a 20 mM constant concentration, with automatic suppression (CSRS suppressor - 2 mm), and with a 0.33 mL min−1 system flow through an IonPac CG-12 guard column (2 x 50 mm) and CS-12 (2 x 250 mm) capillary column. This resulted in a 14 min running time for each injection. For soluble Na, NH4, K, Mg and Ca the detection limits (USEPA, 1997) were 2.0, 1.3, 0.9, 0.7, and 1.8 µg L−1, respectively, and the expanded uncertainties at the 95% level of confidence (BIPM, 2008) were of 9, 7, 21, 11, and 23 %, respectively."

8. In the title of Table 2, it is not "aerosol characterization" it is aerosol composition; it does not correspond to "during the Saharan dust event ", it is before, along and after the event.

R: The reviewer is correct. Table 2 was removed from the text, and essential information was added to Figure 2 and in the text.

9. In Lines 279-282 the authors say that K, Zn and Cu are of biogenic sources, probably mostly emitted during biomass burning. If the detected pulse of dust in this work is coincident with an African biomass burning event as pointed by the authors, what is the level of certainty to say that their main source is the mineral fraction?

R: Biomass burning in Africa could have contributed some Fe, but unfortunately, little is known about Fe emissions from savanna fires, and the available data span a wide range. From the work of Gaudichet et al. (1995), one can derive an Fe content of 0.016% in savanna smoke TPM, which with a peak biomass smoke concentration of 4 µg m^{-3} would only give 0.6 ng Fe m^{-3}. Using the BC/Fe ratio of ca. 40 from Maenhaut et al.

(1996) and the peak BCe concentration of 0.3 μg m^{-3}, we can estimate ca. 8 ng Fe m^{-3}. Finally, using the Fe emission factor of 0.026 g/kg for African savanna fires from Andreae et al. (1998) and the BC emission factor of 0.6 g/kg from Andreae and Merlet (2001 and updates), we can estimate a peak pyrogenic Fe contribution of 13 ng m^{-3}.This compares to 64 ng m^{-3} of soluble iron at the same time, and given that only a small fraction of the Fe in biomass smoke is likely to be soluble, it is clear that the dominant fraction of soluble Fe comes from the African mineral dust.

Discussion on this issue has been added in Section 3.1.

10. In Line 322, the comparison of the present work with Andreae et al. (2015): does both work have same methods and associated errors? Results of Andreae et al. (2015) correspond to what period of the year. Specify please.

R: The results of Andreae et al. (2015) correspond to the period from 7 March to 21 April 2012, and the chromatography analyses have the same method and associated errors. The information was added to the text as follows: (L. 367-369)" The soluble Fe(III) concentrations were significantly higher than those reported by Andreae et al. (2015) from earlier measurements at the same site, which had also been made during the wet season and using the same quantification method."

11. Text in lines 333-338 is unnecessary.

R: We agree with the reviewer, the text was removed.

12. Dates in Figure 2 is unreadable.

R: We agree with the reviewer, the Figure 2 was replaced by another with readable information.

13. Figure 3 should be completely edited. It is not possible to use the Hysplit output directly. For Figure 3, use ensembles, not a single trajectory; a family of trajectories gives a better idea of all geographical contributions.

R: We agree with the reviewer and the figure was edited as requested, showing the backward trajectories to

illustrate the intercontinental transport.

15. Lines 369-374; Figure 1 shows before, along and after the "dust storm", I suggest that the authors run the Hysplit model in these 3 circumstances and then make their conclusions.

R: We agree with the reviewer. Figure 1 was replaced and comments changed with new conclusions added according to the suggestion.

16. In Line 387 provide complete localization of the three AERONET sites: Dakar and Ilorin in Africa, and Embrapa/ Manaus in Amazon.

R: The geographical coordinates of these AERONET sites have been included for the AERONET sites (L. 227): Dakar (14° 23' 38''N; 16° 57' 32''W) and Ilorin (08° 19' 12''N; 04° 20' 24''E) in Africa, and Embrapa/Manaus (02° 53' 12''S; 59° 58' 12''W) in Amazonia (L. 802).

17. In Figure 5, AOD do not distinguish dust from biomass burning products. From the location of higher AODs in the diagrams it seems that your source could have some contribution from biomass burning than mineral dust. Also the results presented in the Hysplit are not totally in accordance to wind flows at the charts at Figure 5. Maybe the source is a net combination of both; I strongly suggest that the authors add a map with fire spots for the period of sampling, so to make better differentiate.

R: Yes, there is clearly a contribution from biomass burning. To clarify the possible contribution of smoke, we added in Figure 6 fire spots observed during the sampling period in both continents, South America and Africa. Over South America, major fire spots areas (Brazilian cerrado ecosystem and the north portion of the continent) are not upwind of the ATTO site, which reduces the site exposure to smoke plumes from these principal regional spots. In Africa, the main fire spots areas are downwind of the Sahara desert, along the west coast of Africa, therefore on the way of the dust flux toward the Tropical Atlantic and South America, which could promote transport of a mixture of smoke and dust. The referee is right, the AOD does not distinguish dust from biomass burning. Thus, observing exclusively the AOD map it is hard to say which is one dominant, dust or smoke. However, from the analysis of the Angstrom Exponent (AE) against AOD measured using data from AERONET sites located in the Sub-Saharan areas with high AOD (Ilorin, Dakar and Cape Verde) it is possible to assess the

dominant aerosol type across west Africa. The AE is close to zero when aerosol plumes are dominated by large particles (e.g., sea salt, soil dust, biogenic) and higher than 1.0 when fine particles (e.g., from biomass burning and fossil fuel combustion) are dominant (Eck et al., 1999). It is well established that an increase in AOD associated with a decrease in AE in the sub-Saharan region is associated with the presence of dust plumes, and the opposite, increase in AE associated with an AOD increase is related to biomass burning plumes (Ogunjobi et al., 2008, Eck et al.1999). Although a contribution from biomass burning smoke is very likely in these areas, the plots of AE against AOD for Dakar, Cape Verde, and particularly Ilorin, during the four periods analyzed in Figure 6 shows that dust plumes clearly dominated during the higher AOD scenarios. The plot for the Ilorin case was included as an example in the manuscript to corroborate that the plume that left Africa towards the Tropical Atlantic and South America was dominated by dust aerosols. The same analysis performed for the AERONET station located in central Amazonia (northwest of Manaus) also suggested that regional AOD increases during the sampling period were dominantly connected with decreases in AE, and thus increased coarse mode particles. This is consistent with Castro Videla et al. (2013), who showed that peaks on AOD in Central Amazonia during the wet season had a significant contribution from coarse mode particles. As discussed in the response to Comment 2 of Reviewer 1, a TPM contribution of about 20% from biomass burning can be estimated.

18. In Figure 6, what is MC? Please, correct the legend of time.

R: MC stands for Mass Concentration. The legend was corrected as indicated.

19. The discussion on fungi is very poor. There is none description of the species nor anything on their biogeography. The lesson of this result is the fact that a more detail aerobiological research should be conducted to be published.

R: The fungi identification underscores long distance transport, but doesn't allude to a specific site. We included our observations of coarse particles during the dust event to see if there were likely to be readily identifiable inputs from the canopy that might add to the iron analysis. Bioaerosol identification would also help confirm if any coarse particles that were mixed with the dust were of other than local origin. The spores identified in the samples do not add soluble iron to the analyzed extracts.

20. In Line 463-465, the authors say "Smoke plumes are known to entrain fungi over long distances (Mims and Mims, 2004). Dust from Lake Chad is rich in bacteria and fungi." Here becomes explicitly that the authors are not able to stablish a source of the particulate matter entering Amazon in the considered event: Saharan mineral dust or sub-Saharan biomass burning?

R: The particles found have influence from the plumes originated from the African continent as confirmed by trajectories. The long distance transport is evidence from our findings but we cannot be more precise about the source of the fungi without further analysis.

21. The Amazon itself is a fantastic source of bacteria and fungi, and only an endemic specie of Africa, detected in Amazon, at high level (ex. The top of the ATTO) could make a clear distinction.

R: The reviewer is correct. We cannot fully compare the bioaerosol results because previous studies cultured air samples of viable spores only, and analysed with high throughput sequencing. Only a few types of fungi were detected at the species level.

22. In item 3.5 the authors says that "a small amount of atmospheric iron could affect the microbiota in the canopy, rather than have a significant effect on soil and root uptake for plants." This is an speculation and from this work it is not possible to conclude anything.

R: Yes, we agree with the reviewer. The sentence was removed and the section restructured to emphasize our finding.

23. In my opinion, most of item 3.5 is Introduction to the study since most of the text is compilation from the literature associated to this work.

R: Yes, we agree with the reviewer. Some parts of section 3.5 were placed in the Introduction and most of the section was rewritten (L. 433-452).

24. The conclusion unrealistic, should be reduced to the basic findings.

R: The conclusion was rewritten to focus on our findings (L. 454-461).

MARKED-UP MANUSCRIPT VERSION:

~~Mineral~~Soluble iron nutrients in Saharan dust ~~and their potential impact on Amazon~~over the central Amazon rainforest ~~ecology~~

Joana. A. Rizzolo[1], Cybelli. G. G. Barbosa[1], Guilherme C. Borillo[1], Ana F. L. Godoi[1], Rodrigo A. F. Souza[2], Rita V. Andreoli[2], Antônio O. Manzi[3], Marta O. Sá[3], Eliane G. Alves[3], Christopher Pöhlker[4], Isabella H. Angelis[4], Florian Ditas[4], Jorge Saturno[4], Daniel Moran-Zuloaga[4], Luciana V. Rizzo[5], Nilton E. Rosário[5], Theotonio Pauliquevis[5], Rosa M. N. Santos[2], Carlos I. Yamamoto[6], Meinrat O. Andreae[4], Paulo Artaxo[7], Philip E. ~~Taylor[7] and~~ Taylor[8] and Ricardo H.M. Godoi[1]

[1] Environmental Engineering Department, Federal University of Parana, Curitiba, PR, Brazil.
[2] State University of Amazonas - UEA, Meteorology Department, Manaus, AM, Brazil.
[3] Instituto Nacional de Pesquisas da Amazônia, Programa de Grande Escala Biosfera Atmosfera na Amazônia, Manaus, Brasil.
[4] Max Planck Institute for Chemistry, Biogeochemistry Department, Mainz, Germany.
[5] Universidade Federal de São Paulo, Instituto de Ciências Ambientais, Químicas e Farmacêuticas, Diadema, Brasil.
[6] Chemical Engineering Department, Federal University of Parana, Curitiba, PR, Brazil.
[7] Institute of Physics, University of São Paulo, São Paulo 05508-900, Brazil
[7,8] Deakin University, CCMB and CMMR, School of Life and Environmental Sciences, Geelong, Vic, Australia.

Correspondence to: Philip E. Taylor (philip.taylor@deakin.edu.au) and Ricardo H.M. Godoi (rhmgodoi@ufpr.br).

Abstract. The intercontinental transport of aerosols from the Saharan ~~is likely to play~~Desert plays a significant role in nutrient cycles in the Amazon rainforest, since it carries many types of minerals to these otherwise low-fertility lands. Iron is one of the micronutrients essential for plant growth, and ~~the~~ its ~~Amazon rainforest is iron limited. The main aim of this study was to assess the input and potential impact of iron bioavailability from Saharan dust, namely, the soluble fraction Fe(II)/Fe(III). Seven other soluble elements that are also essential for plants were measured. Dust particles entrained in the air were collected and analyzed, but not dust deposited in rainfall as atmospheric washout. The sampling campaign was carried out at the ATTO site (Amazon Tall Tower Observatory), from March to April 2015, and samplers were placed both above and below the canopy. Mineral dust aerosol at ATTO showed peak concentrations for Fe(III) (47.6 ng m^{-3}), Fe(II) (16.2 ng m^{-3}), Na (470 ng m^{-3}), Ca (194 ng m^{-3}), K (64.7 ng m^{-3}), and Mg (88.8 ng m^{-3}) during the presence of dust transported from the Sahara, as determined by remote ground based and satellite sensing data and backward trajectories.~~ long-range transport might be an important source for the iron-limited Amazon rainforest. ~~Atmospheric transport of weathered Saharan dust, followed by surface deposition, results in substantial iron bioavailability across the rainforest canopy. The seasonal deposition of dust rich in soluble iron and other minerals is likely to affect both bacteria and fungi within the topsoil and on canopy surfaces, and especially benefit highly bioabsorbent epiphytes, such as lichens. In this~~

scenario, Saharan dust can provide essential macronutrients and micronutrients to plant roots, and also directly to plant leaves. This study assesses the bioavailability of iron Fe (II) and Fe (III) in the particulate matter over the Amazon forest which was transported from the Saharan Desert (for the sake of our discussion, this term also includes the Sahel region). The sampling campaign was carried out above and below the forest canopy at the ATTO site (Amazon Tall Tower Observatory), a near-pristine area in the central Amazon Basin, from March to April 2015. Measurements reached peak concentrations for soluble Fe(III) (48 ng m^{-3}), Fe(II) (16 ng m^{-3}), Na (470 ng m^{-3}), Ca (194 ng m^{-3}), K (65 ng m^{-3}), and Mg (89 ng m^{-3}) during a time period of dust transport from the Sahara, as confirmed by ground-based and satellite remote sensing data and air mass backward trajectories. Dust sampled above the Amazon canopy included primary biological aerosols and other coarse particles up to 12 µm in diameter. Atmospheric transport of weathered Saharan dust, followed by surface deposition, results in substantial iron bioavailability across the rainforest canopy. The seasonal deposition of dust, rich in soluble iron, and other minerals is likely to assist both bacteria and fungi within the topsoil and on canopy surfaces, and especially benefit highly bioabsorbent species. In this scenario, Saharan dust can provide essential macronutrients and micronutrients to plant roots, and also directly to plant leaves. The influence of this input on the ecology of the forest canopy and topsoil is discussed and we argue that this influence would likely be different from that of nutrients from the weathered Amazon bedrock, which otherwise provides the main source of soluble mineral nutrients.

Key words: Amazon forest, SaharaAmazon Tall Tower Observatory, Saharan dust, mineral nutrients, bioavailable, soluble iron, outbreak event, dust bioavailability, long range transport, primary bioaerosols.

1 Introduction

The Sahara is the largest source of desert dust to the atmosphere (Ginoux et al., 2012). Studies are beginning to have revealed the extent of the influence of Saharan dust influence on nutrient dynamics and biogeochemical cycling in both oceanic and terrestrial ecosystems in North Africa and far beyond, due to frequent long-range transport across the Atlantic Ocean, the Mediterranean Sea and the Red Sea, and on to the Americas, Europe and the Middle East (Goudie and Middleton, 2001; Hoornaert et al., 2003, Yu et al., 2015; Longo et al., 2016; Ravelo-Perez et al., 2016; Salvador et al., 2016).

Saharan dust affects climate and atmospheric chemistry at both regional and global scales. Large scale and mesoscale atmospheric circulation have a key role to play in the emission and transport of mineral aerosols. Research is ongoing into the effects of year to year and decade to decade variability of loadings and transport of dust in the atmosphere (Washington and Todd, 2005).

The Amazon Basin, which contains the world's largest rainforest (Garstang et al., 1988; Aragão, 2012; Doughty et al., 2015) receives annually about 28 million tons of African dust each year (Yu et al., 2015), as well as Atlantic sea spray and smoke from African biomass burning (Martin et al., 2010; Baars et al., 2011; Talbot et al., 1990; Andreae et al., 2015).) There have been suggestions that Saharan dust transport across the Atlantic may act as a valuable fertilizer of the Amazon rainforest, providing fundamental nutrients to the Amazon forest (Swap et al., 1992; Koren et al., 2006; Ben-Ami et al.,

2010; Abouchami et al., 2013). However, little is known about the nutrient amounts reaching the Amazon, their bioavailability, ~~of these nutrients~~ and their potential effect on rainforest ecology. It is, therefore, important to understand the source types, source strengths, and the ~~physical and chemical properties~~atmospheric factors that control the solubility of ~~mineral dust aerosol particles~~these minerals over the Amazon Basin.

Plants require many nutrients for healthy development (Marschner, 2012). ~~Iron~~Among several components necessary for plant growth, soluble iron (Fe) is an essential micronutrient ~~for plant growth~~ (Morrissey and Guerinot, 2009) and it is a key element in several important functions and physiological processes. It participates in chlorophyll functioning and is required for enzymes critical for photosynthesis, such as catalase, peroxidase, nitrogenase, and nitrate reductase (Hochmuth, 2011). Other ~~P~~plant bio-functions, such as ~~photosynthesis,~~ respiration and hormonal balance, also require Fe~~, along with other elements~~ (Pérez-Sanz et al., 1995).

~~Under natural soil conditions, Fe(III) occurs bound to minerals, such as hematite, that are not soluble in water (Isaac, 1997; Zhu, 1997), and Fe dissolution is dependent on the water's ligand capacity as well as on than the type or quantity of dust deposited on the surface (Mendez, 2010).~~

Two distinct pathways ~~of Fe uptake~~ have been identified in plant roots for Fe uptake from decomposed litter and weathered bedrock. One present mainly in dicot plants, reduces Fe(III) to Fe(II) by acidification of the rhizosphere. After this reduction, Fe(II) is transported into cells. In the other pathway, compounds with high affinity for iron are secreted into the rhizosphere, where they react with Fe (III) and form a chelate complex. This complex is moved into cells by specific transporters (Hell and Stephan, 2003; Morrissey and Guerinot, 2009). In the forest, microorganisms, such as fungi and bacteria, play a role in nutrient cycling, and often employ multiple distinct iron-uptake systems simultaneously (Philpott, 2006).

~~Furthermore, Fe-rich dust particles can be transported over long distances and have considerable time and surface area to take up acids (An increased proportion of soluble iron has recently been reported in high altitude Saharan dust compared with ground based samples (Ravelo Perez et al., 2016). Thus, particle size, solubility, and bioaccessibility of iron oxides in dust will determine the ultimate influence of these materials on environmental and biological processes (Reynolds, 2014).~~

Besides iron uptake, other elements are also essential for plants. Magnesium (Mg) and Copper (Cu) are required for photosynthesis and protein synthesis. Calcium (Ca) is essential for cell wall and membrane stabilization, osmoregulation, and as a secondary messenger allowing plants to regulate developmental processes in response to environmental stimuli (Gruzak, 2001). Zinc (Zn) is directly involved in the catalytic function of many enzymes, and with regulatory and structural functions (Broadley et al., 2007). Potassium (K) regulates osmotic pressures, stomata movement, cell elongation, cytoplasm pH stabilization, enzymatic activation, protein synthesis, photosynthesis, and transport of sugars in the phloem (Kerbauy, 2012).

Atmospheric mineral dust contributes thousands of tons of minerals to tropical rain forests (Okin et al., 2004; Washington and Todd, 2005; Bristow et al., 2010) and likely contributes to plant nutrition, especially compensating ~~the~~for poor soils with low inherent fertility (Swap et al., 1996). Amazon lowland rainforest soils are shallow and have almost no

soluble minerals; added to this, heavy rains readily leach soluble nutrients from the ground ~~that~~which had been are added from litter decomposition and weathered rocks (Koren et al., 2006).

There are indications that Saharan desert aerosol can compensate ~~for P leaching from~~ for the poor soils of the Amazon (Gross et al., 2015~~). Intercontinental transport of dust is likely to be of great importance to the forest, as it might help to maintain or possibly influence an ecosystem that has roles in global climate regulation, in addition to maintaining regular rainfall and storing vast amounts of carbon (Karanasiou et al., 2012). A number of studies have stated that Saharan dust contributes~~) with phosphorus (P) contributing as a fertilizer to the forest (Swap et al., 1992; Okin et al., 2004; Koren, 2006; Bristow et al., 2010; Martin, 2010; Abouchami et. al, 2013; Yu et al., 2015). ~~Other than for P, the amount of this dust that is available to plants as soluble micronutrients and macronutrients is unknown, as is the potential influence on forest ecology.~~

Under natural soil conditions, Fe(III) occurs bound to minerals, such as hematite, that are not soluble in water (Isaac, 1997; Zhu, 1997) and Fe dissolution is dependent on the water's ligand capacity as well as on the type and quantity of dust deposited on the surface (Mendez, 2010; Shi et al., 2011). An atmospheric process, particle aging, including photoreduction and proton reactions, controls variations in oxidation state, solubility, and bioavailability of iron oxides in dust and determines the ultimate influence these materials have on environmental and biological processes (Siefert et al., 1994; Reynolds, 2014).

Considering that iron is absorbed by plants as soluble Fe~~-~~(II) ~~–~~and Fe~~-~~(III), it is essential to quantify the ~~intake~~ uptake of this ~~mineral~~ element from long-range transported African dust, and evaluate ~~its~~ the potential utilization and effect on the Amazon rainforest as an essential micronutrient. This ~~research~~ study aims to assess the bioavailability of ~~iron, and other elements~~ Fe(II) and Fe~~-~~(III)) in the particulate matter ~~in~~over the Amazon ~~atmosphere~~forest, which was transported ~~within African dust. This is then used to assess the likely effect on rainforest ecology.~~from Africa and particularly from the Saharan Desert.

2 Method

2.1 ~~Dust sampling~~Aerosol sampling

Sampling was performed on a ~~80-m walk-up~~triangular ~~tower~~mast (S 2° 08.602', W 59° 0.0033') at the Amazon Tall Tower Observatory (ATTO) site (Andreae et al., 2015), a research area in the central Amazon Basin with minimal influence of anthropogenic emissions, in particular during the wet season when near-pristine atmosphere conditions are prevalent. The sampling period ranged from 19 ~~–~~March to 25 ~~–~~April 2015, which ~~is within the typical period that~~ dust transport to the Amazon Basin has been ~~observed~~ reported before (Talbot et al., 1990; Swap et al., 1992; Prospero et al., 2014; Yu et al., 2015). ~~Aerosols~~Total particulate matter (TPM) ~~were~~ was sampled above the canopy at 60 m height above ground level (AGL) and below the canopy at 5 m height~~, without size cut-off,~~ (AGL), and transported in a laminar flow through a 2.5 cm diameter stainless steel tube. The aerosol flow was dried by ~~into an air-conditioned container. The sample humidity at 60 m height was kept below 40% using a~~ a ~~silica~~diffusion dryer~~. The sample humidity at 5 m height was kept dry with a silica gel~~

~~diffusion dryer installed on the inlet line~~. Atmospheric particles were collected on ~~Nuclepore®~~ polycarbonate filters (47 mm diameter, 0.8 µm pore size, Whatman® Nuclepore) at a flow rate of 10 ~~l~~± 0.5 L min^{-1}~~min~~$^{+}$.

~~The aerosol~~Due to different activities at the site, the TPM sampling was performed using the inlet below the canopy ~~at~~ (5 m height) for the first 11 days, and the inlet at 60 m height for the other~~s~~ 26 days. ~~The samples~~Samples were collected over 24 or 48 h periods, ~~consecutively,~~ in order to accumulate sufficient mass to be ~~detected~~quantified by ion chromatography ~~-~~(UV-VIS~~.~~ detection). After sampling, the filters were immediately stored in sterile flasks ~~containing~~under refrigeration until laboratory analysis. Each flask contained nitric acid solution (re-filtered HNO_3, 99.5%) at pH 2.2 ± 0 ~~2.5~~.3, in order to ~~interrupt~~quench the ~~transition~~equilibrium process between the two iron oxidative states, ~~(~~Fe(II) and Fe(III)~~),~~ ~~in order~~and to stabilize the iron concentrations~~, according to the methodology adapted from~~ (Siefert, 1998, Bruno et al., 2000, Cwiertny et al., 2008, Trapp et al., 2010).

Some additional samples for X-ray Fluorescence (XRF) analysis were collected at the ZF2 site (S 2° 35.984', W 60° 12.617') in the Amazon rainforest, about 140 km SW of ATTO. Aerosol samples were deposited on 47 mm polycarbonate filters using a Norwegian Institute for Air Research stacked-filter unit. The combination of filters with 0.4 and 8 µm pore sizes allowed the separation between the fine (PM2.5) and coarse (PM10) modes with a flow rate of 17 L min^{-1}.

2.2 Ion chromatography analysis ~~Determination of mineral~~

~~Soluble species were determined by ion chromatography (Dionex, ICS 5000) using conductivity detection for cations and UV-VIS for soluble transition metals. For cation separation, a capillary column CS12A was used, and for transition metals, a CS5A column (calibrated to quantify traces of Fe(II) and Fe(III)). Each analysis occurred in triplicate and all measurements were performed from a standard curve injected under the same conditions as samples, using Chromeleon® software for processing the generated chromatograms.~~

All the analyses were performed on the TPM soluble fraction. Each sampled filter immersed in nitric acid solution was extracted by an ultrasonic bath for 10 mins. The extract of each sample was filtered through a polyvinylidene difluoride (PVDF) sterile membrane, 0.22 µm pore size with a diameter of 25 mm (Millipore, Merck) and analysed by ion chromatography (ICS 5000, Dionex-Thermo Scientific, USA).

For the transition metal quantification and iron speciation, pyridine-2,6-dicarboxylic acid (PDCA) was used as eluent and 4-2-2-pyridyl resorcinol (PAR) was used as a post-column reagent, stabilized by a PC-10 nitrogen pump. The system flow was 0.3 mL min^{-1} through an IonPac CG5A (2 x 50 mm) guard column, CS5A capillary column (2 x 250 mm) and UV-Vis spectrophotometry with detection at 530 nm (Cardellicchio et al., 1997). For soluble Fe(II), Fe(III), Cu, and Zn the detection limits (USEPA, 1997) were 1.7, 0.4, 1.3, and 4.1 µg L^{-1}, respectively and the expanded uncertainties at the 95% level of confidence (BIPM, 2008) were 3, 42, 46, and 56 %, respectively.

For the cation analysis, ultrapure water and methanesulfonic acid (MSA) was used as the eluent at a 20 mM constant concentration, with automatic suppression (CSRS suppressor - 2 mm), and with a 0.33 mL min^{-1} system flow through an IonPac CG-12 guard column (2 x 50 mm) and CS-12 (2 x 250 mm) capillary column. This resulted in a 14 min running time

for each injection. For soluble Na, NH_4, K, Mg and Ca the detection limits (USEPA, 1997) were 2.0, 1.3, 0.9, 0.7, and 1.8 µg L^{-1}, respectively, and the expanded uncertainties at the 95% level of confidence (BIPM, 2008) were of 9, 7, 21, 11, and 23 %, respectively.

2.3 X-ray fluorescence analysis

Energy dispersive X-ray Fluorescence analysis was applied for the determination of the aerosol elemental composition using an Epsilon 5, PANalytical B.V. instrument. The X-ray tube anode operates with accelerating voltages of 25–100 kV and currents of 0.5–24 mA, at a maximum power of 600 W. The primary target is Sc/W, and 11 secondary targets (Mg, Al, Si, Ti, Fe, Ge, Zr, Mo, Ag, CaF_2, and CeO_2) can be used for measuring different ranges of elements. A special tridimensional polarized-beam geometry reduces the incidence of spurious scattered radiation from the X-ray tube into the detector, thus reducing the background and allowing the measurement of trace elements at very low concentrations (1–30 ng cm^{-2}). Further analytical details of the EDXRF analysis are given by Arana et al. (2014).

2.4 Aerosol ~~Particle~~ physical properties

Aerosol ~~particle~~ physical properties were determined at ATTO during the entire campaign at 60 m height. Mass concentration and ~~particle~~ size distribution were measured by an Optical Particle Sizer (OPS, TSI model 3330; size range: 0.3–10 µm)~~, sampling every~~ at 5 min resolution (Andreae et al., 2015). Equivalent black carbon concentrations (BC_e) were obtained by a ~~MAAP (Multi Angle Absorption Photometer), and the spectral dependency of particle absorption coefficients was determined using a 7-wavelength Aethalometer (Model AE33), both with 1 min resolution.~~Multi Angle Absorption Photometer (MAAP, Model 5012, Thermo Electron Group, USA; λ = 670 nm), based on light absorption measurements at 637 nm. An absorption cross section value of 6.6 m^2 g was used for the conversion of measured absorption coefficients into BCe concentrations (Petzold et al., 2005). Soot, mineral dust, and biogenic particles are light absorbers (Moosmüller et al., 2009; 2011; Guyon et al., 2004; Andreae and Gelencsér 2006) and may contribute to the observed BCe signal. The relative contributions of particle sources to BC_e can be investigated by considering the absorption spectral variability, by means of the so called Absorption Ångström Exponent (AAE). Soot from fossil fuel combustion typically shows AAE close to 1.0, while particles impacted by dust emissions show AAE greater than 2 (Bergstrom et al., 2007). Studies indicate that samples impacted by biomass burning aerosols show AAE in the range of 1.5-2.0 (Bergstrom et al., 2007; Rizzo et al., 2011). The spectral dependency of particle absorption coefficients was monitored using a 7-wavelength Aethalometer (Model AE33, Magee Scientific Company, USA, λ = 370, 470, 520, 590, 660, 880, and 950 nm), compensated for filter loading and multiple scattering effects (Rizzo et al., 2011). Particle scattering coefficients were obtained at three wavelengths using an Integrating Nephelometer (Ecotech, model Aurora 3000~~). Details~~), compensated for truncation errors (Müller et al., 2011). All measurements were taken under dry conditions (RH<50%). More details of the instrumentation setup are given by Andreae et al. (2015).

2.5 Characterization of aerosol plume advection ~~2.4 Modeling,~~

To assess advection of the African aerosol plumes heading towards the Amazon during the sampling period, data from multiple platforms (ground-based and orbital remote sensing and ~~meteorological data~~ modelling tools) were integrated in a complementary way. Air mass backward trajectories were calculated using the Hybrid Single Particle Lagrangian Integrated Trajectory (HYSPLIT) Model from the NOAA Air Resource Laboratory, USA, (National Oceanic and Atmospheric Administration), indicating the airflow toward the ATTO site (Draxler and Rolph, 2015). Thus, dust source areas were inferred by tracking individual dust plumes back to their place of origin (Schepanski et al., 2012) as well as determining transport paths. Ten-day backward ~~T~~trajectories were calculated at three different heights within the atmospheric boundary layer (50, 500, and 1000 m) ~~up to 240 h previous~~. Every 24 h from 19 March to 25 April 2015, a trajectory was calculated with a finishing point at the ~~center of the~~ ATTO site (S 2° 08.752', W 59° 00.335'), at ~~19 h~~19:00 (UTC) (i.e., 15:00 local time).

To evaluate Saharan dust outbreak events and transport toward ATTO during the campaign, ground-based and satellite remote sensing products and *in situ* measurements of aerosol particle optical properties were integrated with the atmospheric large-scale wind field. The wind field product was taken from the Modern-ERa Retrospective Analysis (MERRA), a reanalysis data based on the Goddard Earth Observing System Data Assimilation System Version 5 (GEOS-5; ~~;~~ Rienecker et al., 2011). Ground-based and satellite remote-sensing aerosol optical properties, namely Aerosol Optical Depth (AOD), were obtained, respectively, from aerosol products of the AErosol RObotic NETwork (AERONET, Holben et al., 1998) and of the Moderate-Resolution Imaging Spectroradiometer (MODIS) aboard the Terra satellite (Remer et al., 2005). Given the relevance of biomass burning emissions in both regions sub-Sahara and Amazonia, fire spots taken from the MODIS Active Fire Product (http://modis-fire.umd.edu/index.php, (Giglio et al., 2006; Roy et al., 2008) were integrated and analysed with the MODIS AOD field to clarify the role of smoke source regions. ~~Particle optical properties were continuously monitored *in situ* at the ATTO site in 2015 at a height of 55 m. Particle scattering coefficients were measured at three wavelengths using an integrating nephelometer (Ecotech Aurora 3000). Absorption coefficients were measured at 637 nm using a Multi-Angle Aerosol Photometer (MAAP). Particle single scattering albedo was calculated based on measured absorption and scattering retrieved by interpolation at 637 nm. All measurements were taken under dry conditions (RH<50%).~~

M~~icrom~~eteorological data were obtained by sensors installed on the ~~micrometeorological~~ 80 m walkup tower at the ATTO site, detailed elsewhere (Andreae et al., 2015). Daily values were calculated for ~~vertical wind speed median (W),~~ accumulated precipitation (PRP), and average air temperature (Tair).

~~Table 1 shows the sampling frequencies, micrometeorological measurements, sensors (manufacturers), and sensor heights. For the treatment of high frequency data (10Hz), computational routines were used. First, the sonic raw data was reduced to 1 min medians. Subsequently, daily values were calculated.~~

~~Table 1. List of instruments installed on the walk-up tower (adapted from Andreae et al., 2015).~~

~~Sampling frequency~~	~~Measurement~~	~~Instrument used~~	~~Height/Depth (m)~~	~~Unit~~

0.1 s	u, v,w (wind components	3D ultrasonic anemometer (Windmaster, Gill Instruments Ltd.)	81.65; 46.0; 36.0	m/s
60 s	Rainfall	Rain gauge (TB4, Hydrological Services Pty. Ltd.)	81.0	mm
	Air temperature probe	Thermohygrometer (HMP45C, Vaisala, CS215, Rotronic Measurement Solutions)	81.65; 40.0; 36.0	°C

2.5 6 Spore samples

A Sporewatch spore sampler (Burkard Scientific Pty Ltd, UK) was operated onat the walkup tower at 80 m height for 24 h on 16 separate days between 28- March and 23 -April., simultaneously with the TPM sampling.- Particles larger than 2 µm diameter were impacted onto an adhesive-coated tape attached to a drum within the sampler. This tape was removed, mounted onto a microscope slide and examined with an Olympus BX60 light microscope with brightfield optics. Line scans were performed to identify fungi, and counts were averaged over 24 h and expressed per cubic meter of sampled air sampled. All aerosol concentrations are given with respect to air volumes at ambient temperature and pressureImages were captured with a Canon D1200 DSLR camera and edited with Image J software (Schneider et al 2012). Fungal spores, pollen, fern spores, and other coarse bioaerosols were identified morphologically by a certified pollen and spore counter with the US National Allergy Bureau.

3 Results and discussion

The sampling campaign was performed during a typical period for the occurrence of dust transport events in the Amazon forest. Sampling covered a total of 38 days (19 March - 25 April 2015) and 26 samples of particulate matter were collected.

3.1 Evidence for the influence of African air mass advection on the Amazonian aerosol properties

The largest deposition of iron occurs downwind of the main deserts of the world - North Africa and the Middle East (Mahowald et al., 2009). Koren et al. (2006) estimated that between November and March, the Bodélé Depression is responsible for most of the dust that is deposited annually in the Amazon.

Backward trajectories (HYSPLIT model) show the arrival of air parcels in Central Amazonia originating from the Sahara and downwind areas of the desert between 3 and 6 April 2015 (Figure 1), when the highest concentrations of soluble Fe(III),

Fe(II), Na, Ca, K, and Mg in aerosol samples were recorded at the ATTO site. Moreover, high mass concentrations of coarse mode aerosol were measured during this period (Figure 2).

During the campaign period, three major Saharan dust outbreaks occurred, as identified by the AERONET ground based sunphotometers installed at the West African and sub-Saharan sites of Dakar (14° 23' 38''N, 16° 57' 32''W) and in Ilorin (08° 19' 12''N, 04° 20' 24''E). West Africa is also affected by biomass burning emissions at this time of year (Haywood et al., 2008) and therefore a contribution of biomass burning smoke to the Saharan dust outbreaks is likely. However, the decrease seen in the Angstrom Exponent (AE) as AOD increases at Ilorin (Figure 3) and Dakar (not shown) shows that the air parcels across Saharan and Sub-Saharan West Africa during the three dust outbreaks were dominated by coarse mode particles. It is well established that an increase in AOD associated with a decrease in AE in these regions is highly correlated with the presence of dust plumes, and the opposite, an increase in AE associated with an AOD increase is related to biomass burning plumes (Eck et al.1999; Ogunjobi et al., 2008).

Particulate Fe(III) and Fe(II) concentrations increased between 3 and 9 April, simultaneously with an increase in particle absorption and scattering coefficients (Figure 4.a). A decrease was observed in the intrinsic property, single scattering albedo (SSA, Figure 4.b), suggesting the presence of particles that are efficient light absorbers, such as soot from fossil fuel combustion and biomass burning, mineral dust, and biogenic particles. For comparison, Rizzo et al. (2013) reported that a 7% decrease in SSA at another forest site in the central Amazon during the wet season periods proved to be related to advection of African aerosols. The spectral dependency of absorption, AAE, can be used to distinguish between the different sources of light absorbing particles. The elevated AAE values observed between 6 and 10 April (Figure 4.b) contradict the influence of soot from fossil fuel combustion. During the clean periods (25 March to 2 April and 16 to 24 April), dominated by biogenic particles, AAE values were around 1.8, so that this source of particles, ever present at Amazonian forest sites, may not have contributed to the AAE increase between 6 and 10 April.

Therefore, two light absorbing particle sources are left to explain the increase in absorption and AAE values: biomass burning and mineral dust particles. Fire activity is typically low in the central Amazon between November and April, with less than 2 fire spots per 1000 km^2 and day on average (Castro-Videla et al., 2013), which is corroborated by the map of fire spots distribution during the campaign period (Figure 5). On the other hand, fires are numerous in sub-Saharan West Africa during the study season, and long-range transport of biomass smoke from this region has been shown to be an important influence on atmospheric composition in central Amazonia during the wet season (e.g., Talbot et al., 1990; Wang et al., 2016). The peak BC_e concentration during this event was 0.3 $\mu g\ m^{-3}$, and assuming that all of the BC_e truly represents black carbon and using a typical mass fraction of 7% BC in savanna fire smoke (Andreae and Merlet, 2001), we can estimate a maximum smoke TPM burden of ca. 4 $\mu g\ m^{-3}$ (or about 20% of TPM) during the dust event on 4 April which compares to a peak mass concentration of 55 µm m−3.(details follow in section 3.2).

The dominant role of mineral dust in the aerosol burden during this event can also be corroborated by measurements taken during the same period at another rainforest site (ZF2), ca. 140 km downwind of ATTO (P. Artaxo, pers. comm., 2016). Table 1 shows aerosol element concentrations measured at ZF2 before, during, and after this dust event. The PM10

and BC_e concentrations at ZF2 are in close agreement with those at ATTO, and the soil dust elements Al, Si, and Fe show dramatic increases during the event. A biomass smoke contribution is evident from the increase in fine potassium and BC_e. The rather low fine sulphur concentration is evidence of only a minor influence of fossil fuel derived pollution.

Table 1: Element concentrations in aerosols measured at the ZF2 rainforest site before, during and after the dust event of 3-8 April 2015 (in ng m^{-3}). Potassium and sulphur are in the fine fraction (<2.5 µm), the other concentrations in PM10 (P. Artaxo, personal communication, 2016).

	27 Mar - 02 Apr	03 Apr - 08 Apr	09 Apr -15 Apr
PM10	2900	13700	4800
BC_e	43	271	100
K(fine)	5	97	25
S(fine)	22	164	47
Na(total)	3	125	34
Ca(total)	3	150	28
Al(total)	7	677	115
Si(total)	12	1267	232
Fe(total)	4	402	62
Al/Fe	1.75	1.68	1.85

Biomass burning in Africa could also have contributed some of the observed Fe, but unfortunately, little is known about Fe emissions from savanna fires, and the available data span a wide range. From the work of Gaudichet et al. (1995), one can derive an Fe content of 0.016% in savanna smoke TPM, which, at a peak biomass smoke concentration of 4 µg m^{-3}, would only give 0.6 ng Fe m^{-3}. Using the BC/Fe ratio of ca. 40 from Maenhaut et al. (1996) and the peak BC_e concentration of 0.3 µg m^{-3}, we can estimate ca. 8 ng Fe m^{-3}. Finally, using the Fe emission factor of 0.026 g kg^{-1} d.m. for African savanna fires from Andreae et al. (1998) and the BC emission factor of 0.6 g kg^{-1} from Andreae and Merlet (2001 and updates), we can estimate a peak pyrogenic Fe contribution of 13 ng m^{-3}. This compares to 64 ng m^{-3} of soluble iron (details follow in section 3.3) at the same time, and, given that only a small fraction of the Fe in biomass smoke is likely to be soluble, it is clear that the dominant fraction of soluble Fe comes from the African mineral dust. Insoluble iron is also the main Fe component in the total aerosol, as can be seen by comparing the total Fe concentration of 402 ng m^{-3} during the 3-8 April period with the average soluble Fe concentration of ca. 52 ng m^{-3} measured over the same time.

Our conclusion that African dust dominates the aerosol budget during the dust event is in agreement with Castro Videla et al. (2013) who, based on a five-year study, concluded that peaks in AOD in the central Amazon during the wet season had a significant contribution from coarse mode particles, pointing to a major role of African advection. Besides this, during this

second dust outburst event, the wind speed was stronger than during the first event, implying a faster and more efficient particle transport across the Atlantic, counteracting particle deposition and resulting in substantial effects on particle chemical composition and optical properties at the site. Moreover, at the ATTO site, meteorological scenarios during the days when the increase in Fe(III) and Fe(II) concentrations was observed, between 3 and 9 April, were characterized by warmer conditions and the absence of rainfall (Figure 6), which precludes aerosol wet removal.

3.~~1~~ 2 Characterization of particle physical properties

The mass concentration of PM_{10} particles in Amazonia is close to background in most areas throughout the basin during the wet season. Central Amazonia is characterized by a weak influence of anthropogenic emissions and aerosol mass concentrations are low during the wet season - typically 7 μg m^{-3}; even the most impacted areas do not exceed 10 μg m^{-3} due to intensive rain and the corresponding inhibition of biomass burning (Artaxo et al., 2002, Artaxo et al. 2013, Martin et al., 2010). Increased mass concentrations may occur due to African dust events that reach the Amazon forest in this season (Talbot et al., 1990; Martin et al., 2010). ~~The mass concentration of particles over the Amazon Basin in the wet season is typically around 10 μg m^{-3} in locations that are influenced by biomass burning emissions. In the central Amazon, where the influence of biomass burning is less, the mass concentration is even lower. However, elevated concentrations may occur due to African dust events that reach the Amazon forest (Martin et al., 2010).~~ The highest hourly ~~aerosol~~PM_{10} concentration recorded during our entire campaign was around 55 μg m^{-3} at the ATTO site (5th April), with a daily average of 23 μg m^{-3} (Figure ~~1~~2) ~~, and often concentrations were well below 10 μg m^{-3}~~. Previous studies conducted by Worobiec et al. (2007) at a nearby forest site in Balbina, Amazonia, had also detected an abundance of dust particles during the same season (23th ~~—~~to 29th March 1998). Artaxo et al. (2013) observed~~, only trace levels~~ relatively low concentrations (<0.3 μg m^{-3}) of ~~P, K, and Zn~~soil dust elements (Al, Si, Ti, Fe) during the wet season ~~in at the~~a forest site in central ~~Amazon region. These were thought to have a biogenic source~~Amazonia, but acknowledges episodic concentration increases during periods of influence of particle advection from Africa.

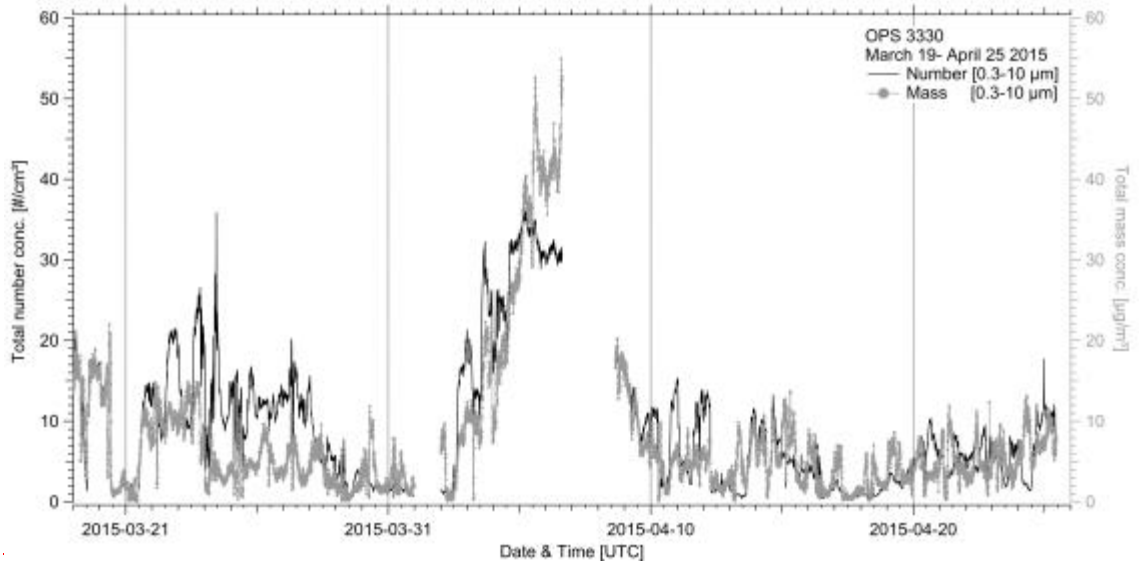

~~Figure 1. Number concentration (solid lines) and mass concentration (dashed lines) time series from the OPS instrument (size range: 0.3-10 µm).~~

For comparison, during Saharan dust events in the Cape Verde archipelago, ~~particulate matter~~PM_{10} concentrations often exceed~~s~~ 100 µg m^{-3}~~-3~~. This is ~~;~~ a relatively high concentration when compared to the ~~average aerosol~~ background level of 10-50 µg m^{-3} (Gross et al., 2015). Obviously, ~~the enhancement in concentrations induced by the~~ a plume ~~is~~has the highest concentrations near the source, so a larger mass of dust is deposited over the Sahara and the adjacent Atlantic than over the Amazon rainforest. Notably, the concentrations at ATTO were still relatively high in view of the large distance from Africa.

The ~~highest~~ concentrations of equivalent black carbon ~~equivalent~~ (BCe) measured online during this intensive campaign ~~were 0.45 µg m-3 (3 April) and 0.37 µg m-3 (~~represented on average 1.5 ~~April). This coincided with the highest~~% of PM10 mass concentrations ~~of particulate matter. The BCe concentrations were retrieved~~, ranging from ~~light absorption measurements. The particle types that mostly contribute~~0 to ~~light absorption are: combustion generated BC, mineral dust, and biogenic particles (Moosmüller et al., 2009; Guyon et al., 2004). Therefore, part of the observed BC could be mineral dust. We further characterized the relative contributions to BCe by considering the Absorption Angstrom Exponents (AAE), which reflect the spectral variability of absorption. Bulk BC particles are expected to have an AAE ?1 due to increased absorption efficiency at shorter wavelengths (<400 nm). The observed variability of AAE is further discussed in section 3.3. During the 2008~~ 0.3 µg m^{-3}. This range is in agreement with previous reports for BCe in the wet season ~~in the central Amazon, at a site near Manaus, BCe concentrations fluctuated between 0.10 and 0.15 µg m-3 (~~at forest sites in the central Amazon (Andreae et al., 2015; Rizzo et al., 2013, Martin et al., 2010). ~~-~~Episodic ~~input~~increases of BCe during the wet season have been attributed to advection of Saharan dust and biomass smoke ~~transported over long distances~~ from Africa ~~explains the presence of BCe detected at ATTO (Andreae et al., 2015).~~in previous studies (Talbot et al., 1990; Andreae et al., 2015; Rizzo et al., 2013; ; Wang et al., 2016). Figure 2 and Table 1 show that BCe concentrations significantly increased regionally

during 1 -8 April, coinciding with the increase in PM10 and particle soluble fraction concentrations and indicating that some biomass smoke (probably from fires in West Africa) arrived together with the dust as discussed in the previous section.

3.2 3 DeterminationComposition of Mineral Aerosol aerosol soluble fraction

The dominant elements in the of the dust samples were Fe(III), Zn, Na, K, and Mg (Table 2). The blank fields in the Table correspond to values below the detection limits, which were calculated according to Method 300.1 USEPA (1997). The expanded uncertainty (ng m^{-3}) was calculated for 95% confidence level, according to BIPM/GUM (2008).

Table 2. Mineral aerosol characterization of 26 samples collected during the Saharan dust event that arrived in the Amazon forest during 2015.

Sampled period (Month/day)	Fe(III) (ng m^{-3})	Fe(II) (ng m^{-3})	Cu (ng m^{-3})	NH_4 (ng m^{-3})	Zn (ng m^{-3})	Na (ng m^{-3})	Ca (ng m^{-3})	K (ng m^{-3})	Mg (ng m^{-3})
3-19	15±0.7	-	-	147±4	105±8	95±7	92±13	54±12	13±2
3-19	11±0.8	-	-	-	14±7	41±6	-	40±8	9.0±1.0
3-20	5.6±0.1	-	-	163±1.7	6.5±3.7	-	-	-	-
3-21	5.8±0.1	-	-	-	3.5±1.8	84±6	40±3	26±3	13±1
3-23	7.1±0.1	-	-	56±2	6.4±3	73±3	-	40±4	10.1±0.5
3-24	4.8±0.1	-	-	33±1	4.2±1.9	25±2	-	29±2	3.0±0.3
3-25	1.8±0.1	-	-	-	2.0±0.9	44±3	-	32±2	6.0±0.6
3-27	2.0±0.1	-	-	-	3.4±1.6	12±1	-	22±2	1.7±0.2
3-28	1.9±0.2	-	0.89±0.87	9.7±1.8	5.0±2.2	18±2	5.9±2.5	25±3	2.6±0.3
3-30	4.1±0.1	-	-	5.2±1.3	5.8±3.8	10±3	-	-	1.2±0.5
3-31	4.1±0.1	-	2.7±0.8	-	4.7±1.9	17±2	-	8.0±5.4	1.7±1.1
4-02	8.5±0.1	-	2.5±1.5	-	8.3±3.7	135±3	12±6	32±4	16±1
4-03	33±0.1	-	-	-	4.6±1.8	441±4	126±4	65±2	67±1
4-05	48±0.1	16±3	-	-	8.4±3.6	470±4	194±4	64±4	89±1
4-06	33±0.1	12±2	0.85±0.75	-	4.3±1.9	220±22	128±8	44±4	49±3
4-08	14±0.2	3.3±3.1	-	16±1	8.9±3.7	148±3	29±4	26±4	244±2
4-09	19±1	1.6±1.6	-	6.6±0.8	5.3±1.9	57±2	29±2	15±2	8.6±0.3
4-11	5.5±0.1	-	-	68±1	9.7±3.7	84±3	-	18±4	8.8±0.5
4-12	5.7±0.2	-	6.4±0.8	-	5.7±1.9	38±2	5.0±1.9	9.6±2.2	5.5±0.2
4-14	6.7±0.2	-	-	20.4±1.19	10.2±3.68	24±3	-	9.4±4.3	3.2±0.5

4-15	12±0.1	-	88±1	98.5±5.45	-	15±2	-	7.4±2.05	10±1
4-17	7.4±0.2	-	9±1	-	10.2±3.9	24±3	-	8.2±4.5	3.7±0.5
4-18	1.1±0.1	-	2.6±0.8	-	4.8±1.7	19±2	3.5±1.7	9.7±2.2	2.7±0.2
4-20	1.2±0.2	-	-	370±1	9.5±3.5	29±3	8.6±3.5	20±4	5±0.6
4-21	2.9±0.2	-	13±0.7	55±1	2.1±1.7	14±2	-	-	4.30±0.2
4-23	2.4±0.1	-	1.0±0.8	-	2.2±1.9	28±2	-	5.4±2.2	3.1±0.3

During the entire sampling period, soluble Na and NH_4 are the dominant cations, and have the highest variation in concentration. Soluble Zn, Na, and Ca exhibit maximum concentrations of 106, 95, and 93 ng m^{-3}, respectively, at 5 m height. During the sampling period between 3 and 10 April, the soluble elements Na, K, Mg, Ca, Fe(III) and Fe(II) showed peak concentrations of 470, 65, 89, 194, 48 and 16 ng m^{-3}, respectively, at 60 m height. For the rest of the period the peak values reached 135, 53, 16, 93 and 15 ng m^{-3}, respectively, and no Fe(II) was measureable. Consequently, the first period cited can be indicative of particulate matter contribution from long distances. The soluble fractions for each element above the canopy from 30 March to 25 April are presented in Figure 7.

The peak concentrations are responsible for the high mean values (black square), except for soluble Zn and Fe(II) (Figure 7). The median values (thick line) for soluble Fe(III), Cu, Zn, Fe(II) and Mg are below 10 ng m^{-3}, while for soluble Na, NH_4, K and Ca the median value is between 10 and 50 ng m^{-3}.

At Bermuda, a location that also receives Saharan dust laden air masses on seasonal cycles, soluble iron was, on average, within the same order of magnitude as at the ATTO site, with mean values ranging from 5 to 9 ng m^{-3} (Longo et al 2016).

The iron in African dust has mixed oxidation states at both ATTO and Bermuda, suggesting that the longer the aerosol remains in the atmosphere, the more reduced the iron becomes. The photoreduction of iron during atmospheric transport and variation in the composition of aerosols could explain this trend (Siefert et al., 1994).

During the wet season in the central Amazon Basin, Artaxo et al. (2002), Martin et al. (2010), and Arana and Artaxo (2014)~~, found similar~~obtained values of total K, Fe, Cu, and Zn in the same as ~~to~~ those found in our ~~campaign.~~investigation. Potassium, ~~K,~~ Cu, and Zn are ~~generally~~ considered to be tracer elements of biogenic emissions from the rainforest~~, although they also have other sources.~~. Potassium in submicron aerosols also has a ~~major~~ source from vegetation fires and is frequently used as a tracer for biomass burning aerosols (Andreae et al., 1983; Martin et al., 2010, Zhang et al., 2015). ~~studied aerosols from a Chinese tropical rainforest, and reported that the high abundance of K in fine particles was likely a result of long range transport from biomass burning.~~

~~Iron, Ti and Al are mainly soil~~Soil dust related elements ~~(Artaxo et al., 1990; Artaxo et al., 1994), and~~ are typically present at the highest concentrations during the early wet-to-dry season transition (~~February to~~ May), as has been shown in previous studies (Pauliquevis et al., 2012; Andreae et al., 2015). This is mainly driven by large-scale atmospheric circulation patterns that favour the transport of dust plumes in a trans-Atlantic airflow from the Sahara and Sahel regions and towards

the Amazon Basin (Artaxo et al., 1990; Formenti et al., 2001; Graham et al., 2003; Martin et al., 2010; Baars et al., 2011; Ben-Ami et al., 2012).

~~During the wet season, the b~~Biogenic aerosols, present above the canopy in the ~~over~~ Amazon~~ia is~~ during the wet season, are overprinted periodically by episodes of intense transatlantic transport, which brings Atlantic marine aerosols in addition to dust and biomass burning emissions (Talbot et al., 1990; Bristow et al., 2010; Andreae et al., 2015). ~~For example,~~ Zhu et al. (1997) studied North African dust entrained in the trade winds over Barbados (Caribbean) in September, and measured Na concentrations of 2.4 to 6.5 µg m^{-3}. Barbados is in a region that receives large amounts of Na~~-~~-enriched marine aerosols ~~due its localization~~. While these concentrations are higher than those recorded in the present study at ATTO (220 to 470 ng m^{-3}), the co-occurrence of elevated concentrations of Na in the central Amazon with ~~and~~ the mineral dust elements, Al, Fe, and Ca, is clear evidence for the marine origin of Na ~~in the central Amazon~~ (Talbot et al., 1990). Andreae et al. (1990) and later Pauliquevis et al. (2012) observed a positive correlation between Na and Cl in rainwater in the Manaus region, a strong indication of sea salt reaching Central Amazonia.

~~Artaxo et al. (1990) studied aerosols from the Amazon Basin and noted that the concentration of total Fe in the fine mode (<2.5 µm) of soil dust were more than 10 times larger in the wet season than in the dry season (101 ng m^{-3} during daytime, 60 ng m^{-3} during the night and 6.5 ng m^{-3} in the dry season).~~ Pauliquevis et al. (2012) also observed increases in the concentration of total Fe with values reaching 60 ng m^{-3} in the fine mode mostly during February to April in the Amazon Basin, with a seasonal~~semester~~ average of 36 ng m^{-3}. They attributed this to episodes of Saharan dust transport.

~~In contrast to the high bulk dust concentrations at Barbados, the Fe~~The soluble Fe(II) concentrations recorded at ATTO during our sampling campaign (1.6 to 16 ng m^{-3}) were significantly higher than ~~the~~ Fe(II) concentrations of 0.63 to 8.2 ng m^{-3} measured in mineral dust particles collected from the marine atmospheric boundary layer at Barbados (Zhu et al., 1997). ~~They showed that~~ In Barbados, only a small fraction of the total iron in aerosol particles was present as Fe(II).

For soluble Fe~~-~~(III), we found concentrations in the range of 1.1 to 48 ng m^{-3}, with the highest concentrations occurring three days in a row (34, 48 and 33 ng m^{-3}). ~~This soluble Fe(III) is carried in dust particles that are mainly deposited onto canopy surfaces by dry sedimentation. Our s~~The soluble Fe(III) concentrations were significantly higher than those reported by Andreae et al. (2015) from earlier measurements at the same site~~. They~~, which had also been made during the wet season and using the same quantification method. Andreae et al. (2015) had measured ~~only~~ 1.8 ng m^{-3} of soluble Fe~~-~~(III) in 120 ng m^{-3} of total Fe ~~and concluded that the aerosol transport of~~at 80 m height. This soluble Fe~~-~~(III) is ~~not likely to have a significant effect on the ecosystem at ATTO.~~carried in dust particles that can be deposited onto canopy surfaces by dry deposition.

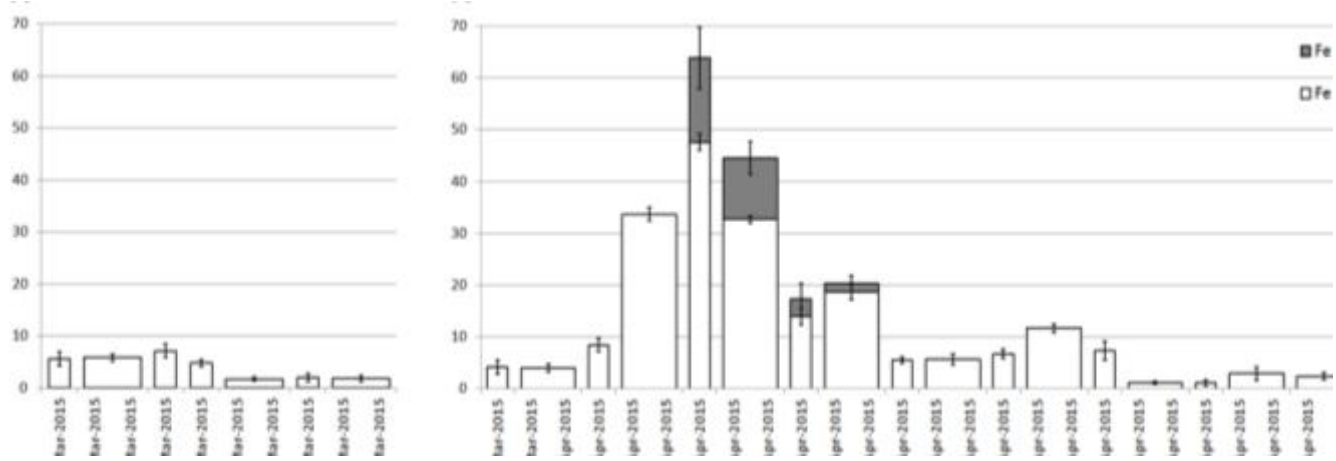

~~Figure 2. Soluble Fe(III) and Fe(II) concentrations in total particulate matter collected during the wet season, (a) sampled at 5 m height (20 March to 29 March 2015) and (b) at 60 m height (30 March to 24 April 2015). The width of bars corresponds to the sampling period: 24 or 48 h.~~

~~Desert dust plumes contain iron mainly in the Fe(III) oxidation state, whereas in industrial effluents Fe is mostly in the Fe(II) oxidation state (Reynolds et al., 2014). These same authors collected dust from the Sydney area (Australia) and strongly suggested that the addition of Fe(II)-bearing minerals was associated with industrial, urban, and transportation sources entrained in dust plumes that originally lacked these minerals.~~

The variation of iron oxidation state in Saharan dust during atmospheric transport could be the effect of atmospheric process during the long oceanic transport, as Fe(II) and Fe(III) have variable susceptibilities to photochemical processes (Longo et al. 2016).

Bristow et al. (2010) ~~analyzed~~ analysed aerosol samples collected from the Bodélé Depression, Chad, and suggested that the amounts of Fe in some samples likely indicate the presence of ferromagnesian minerals and also reflect the presence of Fe oxides such as goethite and hematite, or Fe ~~sulfate~~ sulphate salts that have been detected in Saharan dust.

Abouchami et al. (2013), studying the geochemical characteristics of the Bodélé Depression dust source and the relation ~~with~~ to transatlantic dust transport to the Amazon Basin, found lower Na, K, Fe, and Ca concentrations in Amazon Basin soil samples than in the Bodélé samples, suggesting that this difference is a reflection of remobilization and loss of these elements by chemical weathering under the hot, wet climate conditions in the Amazon Basin.

~~**Modeling, Remote Sensing and Meteorological Data**~~

~~The largest deposition of iron occurs downwind of the main deserts of the world - North Africa and the Middle East (Mahowald et al., 2009). Figure 3 (a and b) shows the backwards trajectories coming not from North Africa nor the Middle East, but instead from the Saharan desert (Formenti et al., 2001; Washington and Todd, 2005; Bristow et al., 2010;~~

Creamean et al., 2013). Koren et al. (2006) estimated that between November and March, the Bodélé Depression is responsible for most of the dust that is deposited annually on the Amazon.

Using backward trajectories data (HYSPLIT model), it is sight a connection between the transport from Sahara to Amazon was estimated. Between 3rd and 6th April, the highest concentrations of Fe (III), Fe (II), Na, Ca, K and Mg in mineral dust samples were observed. According to Figure 3, the air masses arriving in the Amazon during that period originated from the Saharan region.

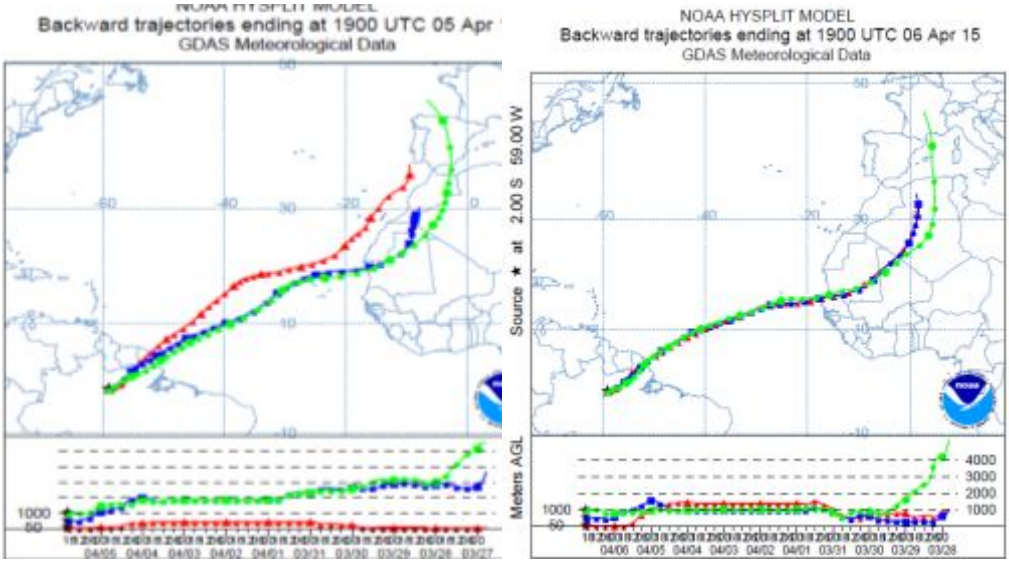

Figure 3. Backward trajectories of air parcels at 50, 500, and 1000 m above the Amazon for 240 h during the sampling periods in which the greatest concentrations of dust from the Sahara arrived at ATTO.

High mass concentrations around 3-8from 3rd to 8th April 2015 coincided with the arrival of African dustaerosol in the Amazon Basin, according to OPS instrumentsaerosol concentrations and backward trajectories, respectively, Figure 1 and 3. Periodically in the wet season, long range transport of sea spray, Saharan dust, and/or smoke from African biomass burning can deposit across the Amazon Basin (Martin et al., , respectively.2010; Baars et al., 2011; Andreae et al., 2015).

As identified by the AERONET ground based sunphotometers located in Dakar and in Ilorin, during the campaign period three major Saharan dust outbreaks occurred and eventually combined with smoke (Figure 4.a).

The first outbreak peaked on 22th March and had a stronger effect on AOD over Ilorin compared to Dakar. This feature was corroborated by the MODIS mean AOD field from 20th to 25th March (Figure 5.a). During this first event, the atmospheric circulation was not able to promote a significant transport of the dust and smoke plume towards South America. The influence of African particle advection on aerosol optical properties observed at ATTO was weak, but still detectable. An increase in absorption and scattering coefficients was observed in comparison to the clean periods (25th March to 2nd April and 16th –24th April), however, no significant increase of AAE observed during this event (Figure 4.b). A less active

dust outbreak from 25th to 30th March followed the first event, as shown by ground based and satellite data (Figure 4.a and 5.b).

A second dust outbreak event started at the beginning of April, according to the AERONET retrievals, and its effects on the African sites extended until 9th April. The satellite mean AOD field during this period (Figure 5.c) revealed a consistent pattern of dust transport towards the northeast portion of the Amazon basin, with the wind flow in the direction of ATTO coming from regions effectively influenced by the Saharan dust plume. It is possible that smoke from biomass burning in the African sub-Sahel region joined with dust aerosols transported to the Amazon, since the Ilorin region is affected by biomass burning emissions in this season (Haywood et al., 2008). Fe(III) and Fe(II) concentrations in particulate matter increased between 3 and 9 April (Figure 2), and this correlated with an increase in particle absorption coefficients and a decrease single scattering albedo (Figure 4.b and 4.c). The AAE during this event reached values higher than 5, and after 10 April returned to background levels. The increase in AAE is a strong indication that dust and/or biomass smoke particles contributed to the observed increases in

absorption coefficients. The correlation between the concentration of crustal elements particulate matter and aerosol absorption coefficients African advection events has also been reported for another forest site in the Amazon (Rizzo et al., 2013). The observed changes in particle optical properties can be explained by the presence of Saharan dust particulate matter and biomass burning from the Sahel region. Beside the appropriate transport direction, during the second event the wind circulation speed was stronger than during the first event. This enhanced the Saharan dust advection toward ATTO and resulted in more substantial effects on particle chemical composition and optical properties at the site.

The third event that began around 10th April and lasted until 17th April, according to the African AERONET sites (Figure 4.a), and was the largest dust outbreak event that occurred during the campaign. This was corroborated by the significant increase registered in the AERONET AOD and by the large values and spread of AOD retrieved by MODIS (Figure 5.d). However, this massive dust transport toward the Atlantic basin did not translate into significant changes in the properties of particles sampled at the ATTO site. As happened in the first dust outbreak event, atmospheric wind circulation prevented the transport of the dust plume in the direction of the ATTO site. At this time, a strong zonal wind (eastward) from the African west coast carried the dust plume core toward the extreme north portion of South America, away from ATTO. Meanwhile, the site received an influx of air mass predominantly from an area southward of the plume.

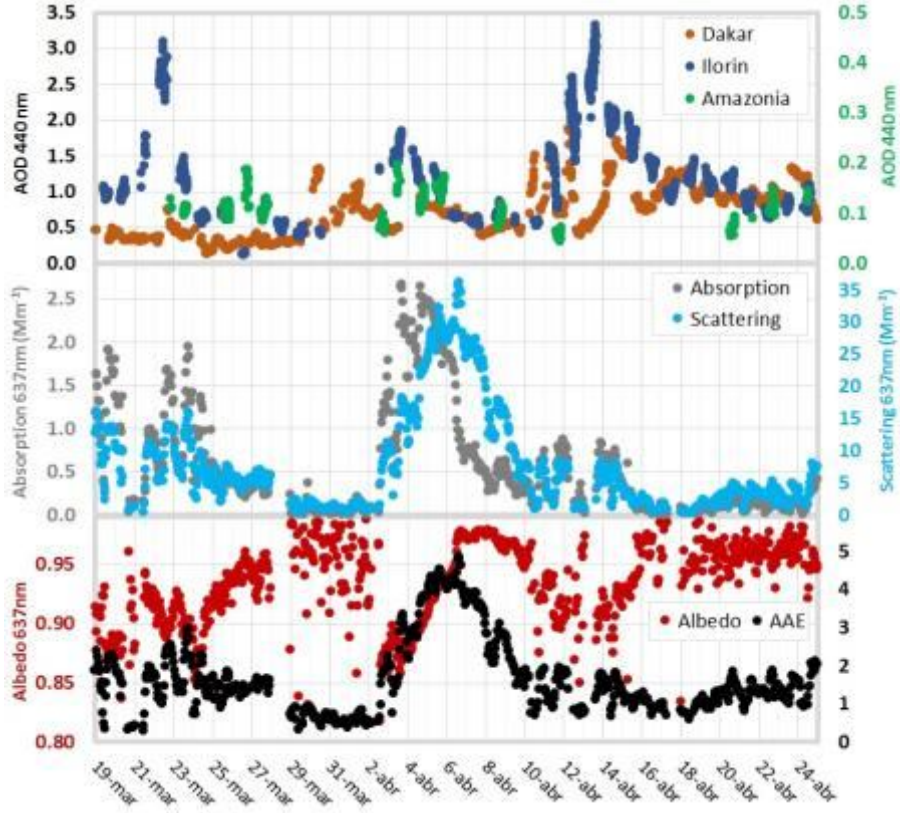

~~Figure 4. a) Instantaneous Aerosol Optical Depth (AOD) at 440 nm measured at three AERONET sites: Dakar and Ilorin in Africa, and Embrapa/Manaus in Amazonia. b) Particle absorption and scattering coefficients at 637 nm observed in situ at the ATTO site. c) Particle single scattering albedo at 637 nm, and Absorption Angstrom Exponent (AAE), retrieved from in situ observations of aerosol optical properties at ATTO.~~

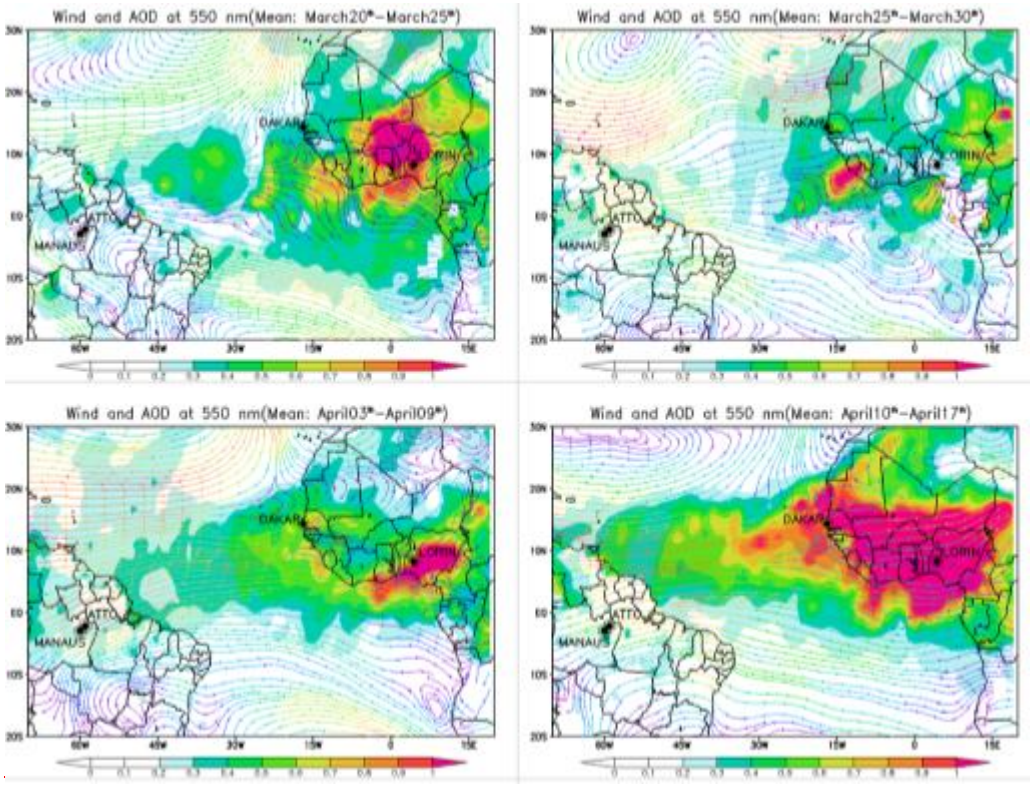

~~Figure 5. Mean distribution of aerosol optical depth at 550 nm (AOD) and wind at 850 hPa for four distinct periods within the campaign at ATTO site, during the dominance of: a) the first Saharan dust outbreak; b) a less active dust outbreak period; c) the second Saharan dust outbreak; d) the third Saharan dust outbreak.~~

~~Figure 6 shows that during days without rainfall, the vertical wind speed, W, was highest above the canopy level (81.65 m), due to the canopy heating the air above it. Without sunlight forcing, W values did not show significant difference at or below the canopy (46 m and 36 m height, respectively). Levels below the canopy were, on average, between a maximum of -0.0012 m/s and minimum of -0.03 m/s, and always negative, although very close to zero.~~

~~At the highest level of W, being positive (ascending air), we also observed the largest values for Fe(III) and MC.~~

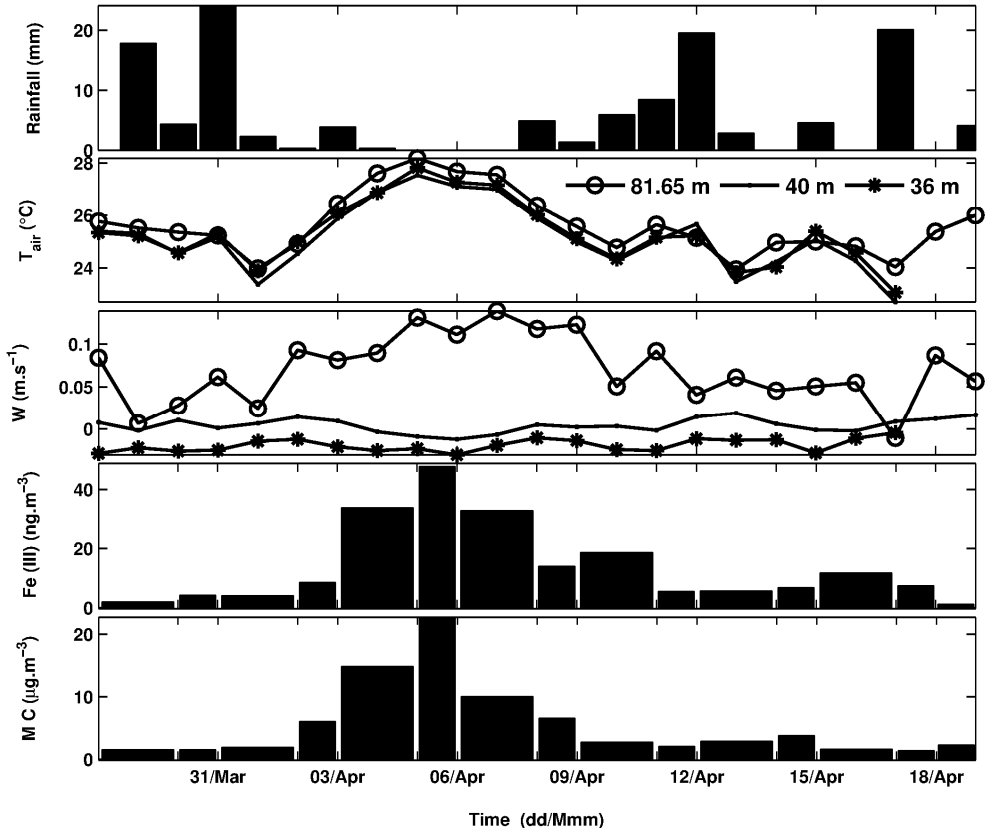

~~Figure 6. Daily comparison of micrometeorological variables (T_{air}, PRP and W) with measurements of Fe(III) and MC below the canopy.~~

3.4 ~~Spore sample~~Coarse particles and bioaerosols above the canopy

Sporewatch sample analysis at ATTO showed that coarse particles, pollen, and fungal spores were common at 80 m height during the African dust plume, whereas very few coarse particles (> 2 µm diameter) had occurred in the atmosphere until 2nd April. On 3rd April at ~~13~~17:00 ~~h~~ (~~LT~~UTC), coarse particles (2 to 10 µm) peaked in number, and were black, hyaline or variously coloured and of irregular shape. The amorphous particles were interspersed with a large diversity of small fungal particles~~.~~ (Figure 8). Fungi that were identified included basidiospores, such as *Ganoderma* and spores from ground-growing coprinoid fungi. Also present were ascospores, asexual conidia, such as *Cladosporium*, ~~Ganoderma,~~ and uni- and bi-cellular hyaline conidia ~~(Figure 7).~~. Several small pollen grains from ground growing herbs of the Apiaceae family were also observed. No moss or fern spores were found. A full quantitative and taxonomic analysis of bioaerosols at select heights above the canopy and throughout the year of 2015 will be reported in a separate study. All ~~fungi detected~~primary biological particles in the sample had a diameter less than 12 µm, similar to adjacent coarse dust particles. At 80 m height, ~~T~~the total fungal count was 1,587 spores per cubic meter of air, averaged over 24 h (2nd ~~—~~to 3rd April). High concentrations of fungi

and other coarse particles persisted in the samples for several days, peaking again at approximately ~~16:30 h (LT)~~20:30 (UTC) on 5th April. From the afternoon of 6th April ~~on,~~onwards, once again very few particles and only the occasional spore were observed.

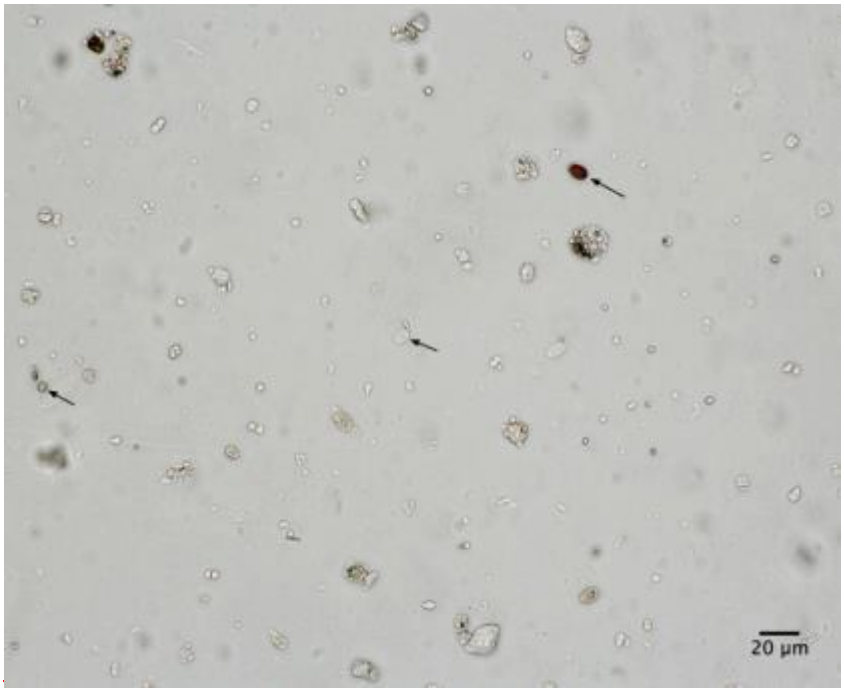

~~Figure 7. Brightfield microscopy of particles collected in an air sampler at 80 m on 2 April 2015. The arrows point to three fungi: the one on the right is a basidiospore, at center is a yeast-like conidia, and at left is a small fungal spore of unknown type.~~

~~As previously discussed, coarse particles observed between 2 and 6 April are likely to be associated with the dust cloud arriving from Africa. The large diversity~~A substantial number of ~~small fungal~~coprinoid spores ~~and conidia entrained in the dust collected at 80 m height~~were identified, but only between 2 and 6 April. ~~are also likely to be sourced to Africa. Smoke plumes are known to entrain fungi over long distances (Mims and Mims, 2004).~~ Coprinoid fungi have not been found in the canopy of rainforests (Mims and Mims, 2004; Prospero et al., 2005; Womack et al., 2015). Instead, they are more common at ground level across arid and temperate zones, consistent with an African source. Otherwise, they might have come from further away in South America, e.g., from clearings in the forest in NE Brazil. Dust from Lake Chad is also rich in bacteria and fungi (Favet et al., 2013). ~~These fungi would have also contributed to the elements detected in air samplers.~~ Bacteria are likely to accompany the dust particles, attached to their surface (Yamaguchi et al., 2012; Prospero et al., 2005~~), but it~~). We cannot fully compare the bioaerosol to determine an African source because previous studies cultured air samples of viable spores only, and analysed them with high throughput sequencing. Only a few types of fungi were detected at the species level in these studies. It is unknown whether any of ~~these organisms~~the fungi observed in the dust above the Amazon are still viable upon sedimentation ~~across~~onto the ~~central Amazon forest.~~forest. Other than during the formation of a Saharan

dust plume, smoke plumes are also known to entrain fungi over long distances (Mims and Mims, 2004), so that some of the fungal material could have been introduced by burning in West Africa.

Up to half of all micronutrients in the canopy are stored in epiphytes (Cardelus, 2010). Fungi housed within lichens take advantage of the large surface area provided by their algal co-host, and are one of the most bio-absorbent organisms evolved for uptake of minerals and other nutrients from atmospheric gases and particulates, and from both dry deposition and rainfall. Another type of fungi common within the Amazon canopy are yeasts, such as Saccharomycetes (Elbert et al., 2007; Womack et al., 2015).

During dry weather, as well as during fog and light rain events, dust deposits onto the canopy and impacts directly onto leaves of vascular plants (e.g., trees and vines), as well as epiphytic vascular and non-vascular plants, such as bryophytes (e.g., lichens, mosses and liverworts). Dust also settles onto ferns, and fungi within the canopy. Air sampled from 40 m height showed that fungi~~~~al material was~~ emitted from ~~are common in~~ the canopy throughout each day and night. The smallest and most metabolically active ~~fungi~~fungal emissions detected in the canopy included lichens and yeasts (Womack et al., 2015).

Up to 25,000 tons of phosphorus has been calculated as being deposited each year on the Amazon. Meanwhile, a similar amount of phosphorus has been estimated to be leached from rainforest soils (Yu et al., 2015). While much of the emphasis has been on soil chemistry and root absorption, water-soluble minerals, as such as P and K, can also be absorbed by leaves (Hochmuth, 2011). Mineral~~s~~ nutrients, such as Fe, can be absorbed through plant leaves as well (Fernandez and Brown, 2013). Thus, canopy deposition of Saharan dust is likely to provide soluble iron to plants via their leaves, in addition to having an influence on epiphytes and surface microorganisms.

3.5 Iron availability

The soluble iron ~~measurement results presented here show a predominance~~measured during the sampling period consisted of about 87% Fe~~~~(III~~) ~~in the samples, while~~) and only 13% Fe~~~~(II)~~, ~~the form which plants can directly absorb,~~and the +II oxidation state was only measurable in four samples. As shown above, soluble iron accounts for only about 13% of the total iron during the dust event. The ~~interest in determining the concentration of Fe(II) in aerosols, besides being the ionic form absorbed by plants, is related to its much higher~~ aerosol iron solubility ~~than Fe(III) (Zhu 1997). However, the efficiency in absorbing iron varies among~~is a key factor in the formation of reactive oxygen species ~~and genotypes, although within plants the main form is Fe(III) (Kerbauy, 2012).Therefore, plants develop specific strategies for Fe uptake (Hell and Stephan, 2003; Morrissey and Guerinot, 2009) and, added to this, abiotic factors such as pH, redox state, and temperature can influence mineral nutrient speciation and solubility, as can biotic factors. Plant roots also can modify the rhizosphere to affect nutrient availability; when challenged with a specific nutrient deficiency, plants can induce high affinity transporters and other mechanisms in their roots, to assist in meeting their mineral nutrient requirements (Grusak, 2001).The~~in the aqueous phase (Longo et al., 2016). The pH of the environment~~al~~ is important for solubility and therefore the availability of iron to microorganisms, as more iron is available~~present~~ in acid soils~~, but Fe is less soluble in neutral or alkaline situations~~

(Isaac, 1997). The majority of Amazon Basin soils are acidic (Schmink and Wood, 1978) and, similar to Fe, Zn is also better absorbed in soils with low pH (Broadley et al., 2007). In contrast, ~~in alkaline soils,~~ the availability of Zn, Fe and Cu is very low in alkaline soils (Marschner, 2012). However, the efficacy of African dust as a fertilizer depends on many factors, such as particulate matter concentration, composition, solubility, and bioavailability of ~~element~~ minerals. In addition, fungi, the most common type of microorganism in the forest (Fracetto et al., 2013), can readily absorb iron, in soluble and insoluble chemical ~~states. Therefore, it is possible that a small amount of atmospheric iron could affect the microbiota in the canopy, rather than have a significant effect on soil and root uptake for plants.~~forms.

Iron availability in the canopy of forests has commonly been found to be limit~~ed~~ing for growth of epiphytes, bacteria, and fungi (Crichton, 2009). ~~Addition of iron can have a variety of effects on plants and fungi, e.g., yeasts grown in iron-limiting culture show a change in metabolism from fermentation to respiration upon the addition of iron (Philpott et al., 2012). The ongoing deposition of micronutrients, such as iron, onto the Amazon biota is likely to increase both epiphytic growth and fungal and bacterial decomposition within the canopy. Previous observations described an increased tree fall rate attributed to an abundance of epiphytes (Swap et al., 1992). Increase in iron bioavailability is also known to increase the wood to root ratio, increase the rate of plant growth, and increase nutrient cycling within a forest (Benzing, 1998; Crichton, 2009; Cardelius,~~ The uptake of iron by plants is more effective through the leaves than the soil (Hochmuth, 2011). In comparison to soil deposition, foliar deposition from dust sedimentation and rainfall washout is likely to be a very effective mode of application for the absorption of soluble iron into the rainforest biota. Therefore, the presence of iron-rich aerosols deposited onto the canopy is likely to at least partially counter the effects of deficiency of this micronutrient. ~~The full extent of the influence of Saharan dust is yet to be determined, although t~~The majority of soluble mineral nutrients ~~available~~ in the Amazon basin soil originated from the gradual weathering of bedrock ~~in the Amazon basin~~ (Abouchami et al., 2013). Thus, the full extent of the influence of Saharan dust is yet to be determined.

4 Conclusion

~~The current deposition of Saharan dust onto the Amazon is providing an iron-rich source of essential macronutrients and micronutrients. The atmospheric deposition of this nutrient-rich dust on the canopy is likely have an influence on rainforest ecology. Previously unconsidered changes are likely occurring in growth patterns and decomposition rates within the canopy, which affect carbon storage, release, and cycling in the Amazon. Overall, this study examined the bioavailability of soluble macro and micronutrients to plants of the Amazon Basin, and reported peaks~~Peaks in soluble Fe(III~~), Fe(II), Na, Ca, K, and Mg during~~) in atmospheric samples at the ATTO tower were traced to a major dust transport event from the Sahara~~n desert~~Desert~~, according to in 2015. Variations in the oxidation state of Fe suggested that a reductive process is taking place during atmospheric transport.

Analyses included meteorological (backward trajectories and wind field), remote sensing (aerosol optical depth), and *in situ* data ~~analysis. In this way, the elemental contents of samples were correlated with the arrival of African aerosols.~~ collection.

Biomass-burning aerosols and primary biological particles accompanied the plume at its peak. The contribution of marine aerosols from the Atlantic Ocean was identified by a peak in Na. The ongoing deposition of Saharan dust across the Amazon rainforest provides an iron-rich source of essential macronutrients and micronutrients during the wet season. ~~In comparison with soil deposition, foliar deposition from dust sedimentation and rainfall washout is likely to be a very effective mode of application for the absorbance of soluble iron into the rainforest biota.~~

~~Our study also reported on the amount of soluble iron in two oxidation states, Fe(II) and Fe(III), to understand how much of this element is bioavailable to the rainforest in the wet season.~~

~~Because these nutrients are added to the Amazon by atmospheric deposition they will likely: 1) directly affect fungi within the canopy, as well as fungal associated epiphytes, such as lichens. 2) have an influence on bacteria, and 3) provide nutrients directly to leaves and roots of other plants.~~

Author contribution

All authors contributed to the work presented in this paper. R.H.M. Godoi, C.G.G. Barbosa, J.A. Rizzolo, A.F.F. Godoi, C. Pöhlker and A.O. Manzi developed the concept, designed the study and the experiments and J. Rizzolo and I.H. Angelis carried them out. C.I. Yamamoto, G. Borillo and A.O. Manzi provided reagents and gave analytical-technical support. P. Artaxo, C. Pöhlker, J. Saturno, D. Moran-Zuloagal and M.O. Sá collected and analy~~z~~sed data. R.H.M. Godoi, C.G.G. Barbosa, J.A. Rizzolo, P.E. Taylor, L.V. Rizzo, N.E. Rosário, L.V. Rizzo, R.A.F. Souza, R.V. Andreoli, R.M.N. Santos, J. Saturno, D. Moran-Zuloaga, P. Artaxo, M.O. Andreae and T. Pauliquevis analys~~z~~ed data. C. Pöhlker, M.O. Andreae, F. Ditas, L.V. Rizzo, E.G. Alves, T. Pauliquevis and P.E. Taylor gave conceptual advice. J.A. Rizzolo prepared the manuscript and, with contributions from C.G.G. Barbosa, A.F.L. Godoi, E.G. Alves, C. Pöhlker, C.I. Yamamoto, J. Saturno, D. Moran-Zuloaga, L.V. Rizzo, N.E. Rosário, T. Pauliquevis, M.O. Andreae, P.E. Taylor and R.H.M. Godoi, discussed the results and implications at all stages.

Acknowledgments

We acknowledge the support of the Fundação de Amparo à Pesquisa do Estado do Amazonas (FAPEAM), Financiadora de Estudos e Projetos (FINEP), Coordenação de Aperfeiçoamento de Pessoal de Nível Superior (CAPES), Conselho Nacional de Desenvolvimento Científico e Tecnológico (CNPq) and the Fundação Araucária de Apoio ao Desenvolvimento Científico e Tecnológico do Paraná (FA). ~~and the Financiadora de Estudos e Projetos (FINEP).~~ We acknowledge logistical support from the Central Office of the Large Scale Biosphere Atmosphere Experiment in Amazonia (LBA), the Instituto Nacional de Pesquisas da Amazônia (INPA) and the Universidade do Estado do Amazonas (UEA). We also thank the Max Planck Society and INPA for continuous support. We acknowledge the support by the German Federal Ministry of Education and Research (BMBF contract 01LB1001A) and the Brazilian Ministério da Ciência, Tecnologia e Inovação (MCTI/FINEP contract 01.11.01248.00) as well as the UEA, FAPEAM, LBA/ INPA and SDS/CEUC/RDS-Uatumã. We would like to especially thank all the people involved in the logistical support of the ATTO project, in particular Reiner Ditz and Hermes

Braga Xavier. We acknowledge the micrometeorological group of the INPA/LBA for their collaboration concerning the meteorological parameters, with special thanks to Marta Sá and Antonio Huxley. The authors would like to thank Dr. Jose Henrique Pereira from Lawrence Berkeley National Laboratory for the enthusiastic and helpful suggestions.

References

Abouchami, W., Näthe, K., Kumar, A., Galer, S. G., Jochum, K. P., Williams, E., Horbe, A. M. C., Rosa, J. W. C., Balsam, W., Adams, D., Mezgeri, K. and Andreae, M. O.: Geochemical and isotopic characterization of the Bodélé Depression dust source and implications for transatlantic dust transport to the Amazon Basin, Earth and Planet~~ary~~ Sci~~ence~~ Lett~~ers~~, 380, 112-123, doi:10.1016/j.epsl.2013.08.028, 2013.

Andreae, M. O.: Soot carbon and excess fine potassium: Long-range transport of combustion-derived aerosols, Science, 220, 1148-1151, 1983.

Andreae, M. O., Talbot, R. W., Berresheim, H., and Beecher, K. M., Precipitation chemistry in central Amazonia: J. Geophys. Res., 95, 16,987-16,999, 1990.

Andreae, M. O., Andreae, T. W., Annegarn, H., Beer, F., Cachier, H., Elbert, W., Harris, G. W., Maenhaut, W., Salma, I., Swap, R., Wienhold, F. G., and Zenker, T., Airborne studies of aerosol emissions from savanna fires in southern Africa: 2. Aerosol chemical composition: J. Geophys. Res., 103, 32,119-32,128, 1998.

Andreae, M. O., and Merlet, P., Emission of trace gases and aerosols from biomass burning: Global Biogeochemical Cycles, 15, 955-966, 2001.

Andreae, M. O. and Gelencsér, A.: Black carbon or brown carbon? The nature of light-absorbing carbonaceous aerosols, Atmos. Chem. and Phys., 6, 3131–3148, 2006.

Andreae, M. O., Acevedo, O. C., Araújo, A., Artaxo, P., Barbosa, C. G. G., Barbosa, H. M. J., Brito, J., Carbone, S., Chi, X., Cintra, B. B. L., Silva, N. F., Dias, N. L., Dias-Júnior, C. Q., Ditas, F., Ditz, R., Godoi, A. F. L., Godoi, R. H. M., Heimann, M., Hoffmann, T., Kesselmeier, J., Könemann, T., Krüger, M. L., Lavric, J. V., Manzi, A. O., Lopes, A. P., Martins, D. L., Mikhailov, E. F., Moran-Zuloaga, D., Nelson, B. W., Nölscher, A. C., Nogueira, D. S., Piedade, M. T. F., Pöhlker, C., Pöschl, U., Quesada, C. A., Rizzo, L. V., Ro, C.-U. Ruckteschler, N., Sá, L. D. A., Oliveira Sá, M. C. B., Sales, R. M. N., Santos, J., Saturno, J., Schöngart, M., Sörgel, Souza, C. M., Souza, R. A. F., Su, H., Targhetta, N., Tóta, J., Trebs, I., Trumbore, S., Eijck, A van, Walter, D., Wang, Z., Weber, B., Williams, J., Winderlich, J., Wittmann, F., Wolff, S. and Yáñez-Serrano, A. M.: The Amazon Tall Tower Observatory (ATTO): overview of pilot measurements on ecosystem

ecology, meteorology, trace gases, and aerosols, Atmos. Chem. Phys., 15, 10723-10776, doi:10.5194/acp-15-10723-2015, 2015.

Aragão, L. E. O. C.: The rainforest's water pump, Nature, 489, 7415, 217-218, doi:10.1038/nature11485, 2012.

Arana, A. and Artaxo, P.: Composição elementar do aerossol atmosférico na região central da Bacia Amazônica, Química Nova, 37~~(2)~~, 268-276, 2014.

Arana, A., Loureiro, A. L., Barbosa, H. M. J., Van Grieken, R., and Artaxo, P., Optimized energy dispersive X-ray fluorescence analysis of atmospheric aerosols collected at pristine and perturbed Amazon Basin sites: X-Ray Spectrometry, 43, 228-237, doi:10.1002/xrs.2544, 2014.

Artaxo, P. and Maenhaut, W.: Trace element concentrations and size distributions of biogenic aerosols from the Amazon Basin during the wet season, Nucl. Instrum. Methods Phys. Res., 49, 366-371, doi:10.1016/0168-583X(90)90277-2, 1990.

Artaxo, P., Gerab, F., Yamasoe, M. A. and Martins, J. V.: Fine mode aerosol composition at three long-term atmospheric monitoring sites in the Amazon Basin, J. Geophys. Res., 99, 22,857-22,868, doi:10.1029/94JD01023, 1994.

Artaxo, P., Martins, J. V., Yamasoe, M. A., Procópio, A. S., Pauliquevis, T. M., Andreae, M. O., Guyon, P., Gatti, L. V. and Leal, A. M. C.: Physical and chemical properties of aerosols in the wet and dry seasons in Rondônia, Amazonia, J~~ournal of~~ Geophys~~ical~~ Res~~earch~~, 107(D20), 8081, doi:10.1029/2001JD000666, 2002.

Artaxo P., Rizzo, L. V., Brito, J. F., Barbosa, H. M. J., Arana A., Sena E. T., Cirino G. G., Bastos W., Martins S. T. and Andreae M. O.: Atmospheric aerosol in Amazonia and land use change: from natural biogenic to biomass burning conditions, Faraday Disc~~uss.~~, 165, 203-235, doi:10.1039/C3FD00052D, 2013.

Baars, H., Ansmann, A., Althausen, D., Engelmann, R., Artaxo, P., Pauliquevis T. and Souza R.: Further evidence for significant smoke transport from Africa to Amazonia, Geophys. Res. Lett., 38, 1-6, doi:10.1029/2011GL049200, 2011.

Ben-Ami, Y., Koren I., Rudich Y., Artaxo P., Martin S T., and Andreae M. O.: Transport of North African dust from the Bodélé depression to the Amazon Basin: a case study, Atmos. Chem. Phys., 10, 7533-7544, doi:10.5194/acp-10-7533-2010, 2010.

~~Benzing, D. H.: Vulnerabilities of tropical forests to climate change: the significance of resident epiphytes. Clim. Chang. 39, 519-540, doi:10.1023/A:1005312307709, 1998.~~

Bergstrom, R. W., Pilewskie, P., Russell, P. B., Redemann, J., Bond, T. C., Quinn, P. K. and Sierau, B.: Spectral absorption properties of atmospheric aerosols, Atmos. Chem. and Phys. Disc., 7, 10669–10686, doi: 10.5194/acpd-7-10669-2007, 2007.

BIPM.: Evaluation of measurement data – Guide to the expression of uncertainty in measurement JCGM 100:2008 (GUM 1995 with minor corrections), Paris: BIPM Joint Committee for Guides in Metrology, 2008.

Bristow, C. S., Hudson-Edwards, K. A. and Chappell, A.: Fertilizing the Amazon and equatorial Atlantic with West African dust, Geophys. Res. Lett., 37, L14807, doi:10.1029/2010GL043486, 2010.

Broadley, M. R, White, P. J, Hammond, J. P, Zelko, I. and Lux, A.: Zinc in plants. New Phytol., 173, 677-702, doi:10.1111/j.1469-8137.2007.01996.x, 2007.

Bruno, P., Caselli, M., Gennaro, G., Ielpo, P. and Traini, A.: Analysis of heavy metals in atmospheric particulate by ion chromatography, J. Chromatogr A., 888, 145-150, doi:10.1016/S0021-9673(00)00503-3, 2000.

Cardellicchio, N., Ragone, P., Cavalli, S. and Riviello, J.: Use of ion chromatography for the determination of transition metals in the control of sewage-treatment plant and related waters, J. Chromatogr A, 770, 185-192, doi:10.1016/S0021-9673(97)00086-1, 1997.

Cardelus, C. L.: Litter decomposition within the canopy and forest floor of three tree species in a tropical lowland rain forest, Costa Rica, Biotropica, 42, 300-308, doi:10.1111/j.1744-7429.2009.00590.x, 2010.

Castro Videla, F., Barnaba, F., Angelini, F., Cremades, P., & Gobbi, G. P.: The relative role of amazonian and non-amazonian fires in building up the aerosol optical depth in South America: A five year study (2005-2009), Atmos. Res., 122, 298–309, doi: 10.1016/j.atmosres.2012.10.026, 2013.

~~Creamean, J.Cazorla, A., DeMott, P. J., Sullivan, R. C., White, A. B., Ralph, F., Minnis, P., Comstock, J. M. Tomlinson, J. M., and Prather, K. A.: Dust and Biological Aerosols from the Sahara and Asia Influence Precipitation in the Western U.S. Science, 339, 1572, doi:10.1126/science.1227279, 2013.~~

Crichton R.: Inorganic biochemistry of iron metabolism: from molecular mechanisms to clinical consequences, 3rd Ed, Chichester: John Wiley and Sons, pp 461, doi:10.1002/9780470010303, 2009.

Cwiertny, D. M., Baltrusaitis, J., Hunter, G. J., Laskin, A., Scherer, M. M. and Grassian, V. H.: Characterization and acid-mobilization study of iron-containing mineral dust source materials, J. Geophys. Res., 113, D05202, doi:10.1029/2007JD009332, 2008.

Doughty, C. E., Metcalfe, D. B., Girardin, C. A. J., Amézquita, F. F., Cabrera, D. G., Huaraca Huasco, W., Silva-Espejo, J. E., Araujo-Murakami, A., Costa, M. C., Rocha, W., Feldpausch, T. R., Mendoza, A. L. M., Costa, A. C. L., Meir, P., Phillips, O. L. and Malhi, Y.: Drought impact on forest carbon dynamics and fluxes in Amazonia, Nature. 519, 78-82, doi:10.1038/nature14213, 2015.

Draxler, R. R. and Rolph, G. D.: HYSPLIT (Hybrid Single-Particle Lagrangian Integrated Trajectory) Model access via NOAA ARLREADY Website, available at: http://www.arl.noaa.gov/ready/hysplit4.html (last access: 15 October 2016), NOAA Air Resources Laboratory, Silver Spring, MD., 2015.

Eck, T. F., Holben, B. N., Reid, J. S., Dubovik, O., Smirnov, A., O'Neill, N. T., Slutsker, I., and Kinne, S.: Wavelength dependence of the optical depth of biomass burning, urban, and desert dust aerosols, J. Geophys. Res., 104, 31333–31349, doi:10.1029/1999jd900923, 1999.

Elbert, W., Taylor, P. E., Andreae, M. O. and Pöschl, U.: Contribution of fungi to primary biogenic aerosols in the atmosphere: wet and dry discharged spores, carbohydrates, and inorganic ions, Atmos. Chem. Phys.7, 4569-88, doi:10.5194/acp-7-4569, 2007.

Favet, J., Lapanje, A., Giongo, A., Kennedy, S., Aung, Y., Cattaneo, A., Davis-Richardson, A. G., Brown, C. T., Kort, R., Brumsack, H., Schnetger, B., Chappell, A., Kroijenga, J., Beck, A., Schwibbert, K., Mohamed, A. H., Kirchner, T., Quadros, P. D., Triplett, E. W., Broughton, W. J. and Gorbushina, A. A.: Microbial hitchhikers on intercontinental dust: catching a lift in Chad, The ISME Journal, 7, 850-867, doi:10.1038/ismej.2012.152, 2013.

Fernandez V. and Brown P.: From plant surface to plant metabolism: the uncertain fate of foliar applied nutrients, Front. Plant Sci., 4, 289, doi:10.3389/fpls.2013.00289, 2013.

Fracetto, G. M., Azevedo, L. C. B., Fracetto, F. J. C., Andreote, F. D., Lambais, M. R. and Pfenning, L. H.: Impact of Amazon land use on the community of soil fungi, Sci. Agric. 70, 2, 59-67, doi:10.1590/S0103-90162013000200001, 2013.

Formenti, P., Andreae, M. O., Lange, L., Roberts, G., Cafmeyer, J., Rajta, I., Maenhaut, W., Holben, B. N., Artaxo, P. and Lelieveld, J..: Saharan dust in Brazil and Suriname during the Large-Scale Biosphere-Atmosphere Experiment in Amazonia (LBA)-Cooperative LBA Regional Experiment (CLAIRE) in March 1998, J. Geophys. Res., 106, 14919-14934, doi:10.1029/2000JD900827, 2001.

Garstang, M., Scala, J., Greco, S., Harris, R., Beck, S., Browell, E. Sacuse, G., Gregory, G., Hill, G., Simpson, J., Tao, W. and Torre, A.: Trace gas exchange and convective transports over the Amazonian rainforest, J. Geophys. Res., 93, 1528-1550, doi:10.1029/JD093iD02p01528, 1988.

Gaudichet, A., Echalar, F., Chatenet, B., Quisefit, J. P., Malingre, G., Cachier, H., Buat-Ménard, P., Artaxo, P., and Maenhaut, W., Trace elements in tropical African savanna biomass burning aerosols: J. Atmos. Chem., 22, 19-39, 1995.

Giglio, L., Csiszar, I., Justice, C.O.: Global distribution and seasonality of active fires as observed with the Terra and Aqua MODIS sensors, J. Geophys. Res.- Biogeosciences, 111, G02016, doi:10.1029/2005JG000142, 2006.

Ginoux, P., Prospero, J. M., Gill, T. E., Hsu, N. C. and Zhao, M.: Global-scale attribution of anthropogenic and natural dust sources and their emission rates based on MODIS Deep Blue aerosol products, Rev. Geophys., 50, RG3005, doi:10.1029/2012RG000388, 2012.

Goudie, A.S. and Middleton, N.J.: Saharan dust storms: nature and consequences, Earth-Sci. Rev., 56, 179-204, doi:10.1016/S0012-8252(01)00067-8, 2001.

Graham, B., Guyon, P., Taylor, P. E., Artaxo, P., Maenhaut, W., Glovsky, M. M., Flagan, R. C. and Andreae, M. O.: Organic compounds present in the natural Amazonian aerosol: Characterization by gas chromatography-mass spectrometry, J. Geophys. Res., 108, 4766, doi:10.1029/2003JD003990, 2003.

Gross, A., Goren, T., Pio, C., Cardoso, J., Tirosh, O., Todd, M. C., Rosenfeld, D., Weiner, T., Custódio, D., and Angert, A.: Variability in Sources and Concentrations of Saharan Dust Phosphorus over the Atlantic Ocean, Environ. Sci. Technol. Lett., 2 (2), 31-37, doi:10.1021/ez500399z, 2015.

Gruzak, M. A.: Plant Macro- and Micronutrient Minerals Encyclopedia of Life Sciences Nature Publishing Group, doi:10.1038/npg.els.0001306, 2001.

Guyon, P., Graham, B., Roberts, G. C., Mayol-Braceroa, O. L., Maenhaut, W., Artaxo, P., and Andreae, M. O.: Sources of optically active aerosol particles over the Amazon forest, Atmos. Environ., 38, 1039-1051, doi:10.1016/j.atmosenv.2003.10.051, 2004.

Haywood, J. M., Pelon, J., Formenti, P., Bharmal, N., Brooks, M., Capes, G., Chazette, P., Chou, C., Christopher, S., Coe, H. and Cuesta, J.: Overview of the dust and biomass-burning experiment and African monsoon multidisciplinary analysis special observing period, J.~~ournal of~~ Geophys.~~ical~~ Res.~~earch~~: Atmos.~~pheres~~, 113(D23), doi:10.1029/2008JD010077, 2008.

Hell, R. and Stephan U. W.: Iron uptake, trafficking and homeostasis in plants, Planta, 216, 541-551, doi:10.1007/s00425-002-0920-4, 2003.

Hochmuth, G.: Iron (Fe) nutrition in Plant U.S. Department of Agriculture, UF/IFAS Extension Service, University of Florida, IFAS Document SL353, 2011.

Holben, B. N., Eck, T. F., Slutsker, I., Tanré, D., Buis, J. P., Setzer, A., Vermote, E., Reagan, J. A., Kaufman, Y. J., Nakajima, F., Lavenu, F., Jankowiak, I. and Smirnov, A.: AERONET - A federated instrument network and data archive for aerosol characterization, Rem. Sens. Environ., 66, 1-16, doi:10.1016/S0034-4257(98)00031-5, 1998.

Hoornaert, S., Godoi, R. H. M., and Grieken, R. V.: Single particle characterization of aerosol in the marine boundary layer and free troposphere over Tenerife, NE Atlantic, during ACE-2, J. Atmos. Chem., 46, 271-293, doi:10.1023/A:1026383403878, 2003.

Isaac, S.: Iron is relatively insoluble and often unavailable in the natural environment: How do fungi obtain sufficient supplies?, Mycologist, 11, 41-42, 1997.

~~Karanasiou, A., Moreno, N., Moreno, T., Viana, M., Leeuw, F., and Querol, X.: Health effects from Sahara dust episodes in Europe: Literature review and research gaps. Environ. Int., 47, 107-114, doi:10.1016/j.envint.2012.06.012, 2012.~~

Kerbauy, G. B.: Fisiologia Vegetal. 2ª ed, Rio de Janeiro: Guanabara Koogan, pp 431, 2012.

Koren, I., Kaufman, Y. J., Washington, R., Todd, M. C., Rudich, Y., Martins, J. V. and Rosen-feld, D.: The Bodélé depression: a single spot in the Sahara that provides most of the mineral dust to the Amazon forest, Environ. Res. Lett., 1, 1-5, doi:10.1088/1748-9326/1/1/014005, 2006.

Longo, A. F., Feng, Y., Lai, B., Landing, W. M., Shelley, R. U., Nenes, A., Mihalopoulos, N., Violaki, K. and Ingall, E. D.: Influence of Atmospheric Processes on the Solubility and Composition of Iron in Saharan Dust, Environ. Sci. Technol., 50 (13), 6912-6920, doi: 10.1021/acs.est.6b02605, 2016.

Maenhaut, W., Salma, I., Cafmeyer, J., Annegarn, H. J., and Andreae, M. O., Regional atmospheric aerosol composition and sources in the Eastern Transvaal, South Africa, and impact of biomass burning: J. Geophys. Res., 101, 23,631-23,650, 1996.

Mahowald, N. M., Engelstaedter, S., Luo, C., Sealy, A., Artaxo, P., Benitez-Nelson, C., Bonnet, S., Chen, Y., Chuang, P. Y., Cohen, D. D., Dulac, F., Herut, B., Johansen, A. M., Kubilay, N., Losno, R., Maenhaut, W., Paytan, A., Prospero, J. M., Shank, L. M. and Siefert, R. L.: Atmospheric Iron Deposition: Global Distribution, Variability, and Human Perturbations, Annu. Rev. Mar. Sci., 1, 245-78, doi:10.1146/annurev.marine.010908.163727, 2009.

Marschner, H.: Mineral nutrition of higher plants, Academic Press, London, pp 672, 2012.

Martin, S. T., Andreae M. O., Artaxo P., Baumgardner D., Chen Q., Goldstein A. H., Guenther, A., Heald C. L., Mayol-Bracero, O. L., McMurry, P. H., Pauliquevis, T., Poschl, U., Prather, K. A., Roberts, G. C., Saleska, S. R., Silva Dias, M. A.,

Spracklen, D. V., Swietlicki, E. and Trebs I.: Sources and properties of Amazonian aerosol particles, Rev. Geophys., 48, RG2002, doi:10.1029/2008RG000280, 2010.

Mendez, J., Guieu, C. and Adkins, J.: Atmospheric input of manganese and iron to the ocean: Seawater dissolution experiments with Saharan and North American dusts, Mar. Chem., 120, 34-43, doi:10.1016/j.marchem.2008.08.006, 2010.

Mims, S. A. and Mims, F. M.: Fungal spores are transported long distances in smoke from biomass fires, Atmos. Environ., 38, 5, 651-655, doi:10.1016/j.atmosenv.2003.10.043, 2004.

Moosmüller, H., Chakrabarty, R. K. and Arnott, W. P.: Aerosol light absorption and its measurement: A review, J.~~ournal of~~ Quant.~~itative~~ Spec.~~troscopy and~~ Rad.~~iative~~ Trans.~~fer~~, 110(11), 844–878, doi: 10.1016/j.jqsrt.2009.02.035, 2009.

Moosmüller, H., Chakrabarty, R. K., Ehlers, K. M. and Arnott, W. P.: Absorption Ångström coefficient, brown carbon, and aerosols: basic concepts, bulk matter, and spherical particles, Atmos.~~pheric~~ Chem.~~istry~~ and Phys.~~ics~~, 11~~(3)~~, 1217-1225, doi.org/10.5194/acp-11-1217-2011, 2011.

Morrissey, J. and Guerinot, M. L.: Iron uptake and transport in plants: The good, the bad, and the ionome, Chem. Rev., 109, 10, 4553-4567, doi:10.1021/cr900112r, 2009.

~~Okin, G. S., Mahowald, N., Chadwick, O. A. and Artaxo, P.: Impact of desert dust on the biogeochemistry of phosphorus in terrestrial ecosystems, Global Biogeochem. Cycles, 18, GB2005, doi:10.1029/2003GB002145, 2004.~~

Muller, T., Laborde, M., Kassell, G. and Wiedensohler, A.: Design and performance of a three-wavelength LED-based total scatter and backscatter integrating nephelometer, Atmos. Meas. Tech., 4, 1291–1303, doi: 10.5194/amt-4-1291-2011, 2011.

Ogunjobi, K.O., He, Z., Simmer, C.: Spectral aerosol optical properties from AERONET Sunphotometric measurements over West Africa, Atmos. Res., 88, 89-107, 2008.

Okin, G. S., Mahowald, N., Chadwick, O. A. and Artaxo, P.: Impact of desert dust on the biogeochemistry of phosphorus in terrestrial ecosystems, Global Biogeochem. Cycles, 18, GB2005, doi:10.1029/2003GB002145, 2004.

Pauliquevis, T., Lara, L. L., Antunes, M. L. and Artaxo, P.: Aerosol and precipitation chemistry measurements in a remote site in Central Amazonia: the role of biogenic contribution, Atmos. Chem. Phys., 12, 4987-5015, doi:10.5194/acp-12-4987, 2012.

Pérez-Sanz, A. and Lucena, J. J.: Synthetic iron oxides as sources of Fe in a hydroponic culture of sunflower, In: ABADIA, J. Iron nutrition in soils and plants, Dordrecht: Kluwer Academic, 241-246, doi:10.1007/978-94-011-0503-3_35, 1995.

Petzold, A., Schloesser, H., Sheridan, P., Arnott, W. P., Ogren, J. and Virkkula, A.: Evaluation of Multiangle Absorption Photometry for Measuring Aerosol Light Absorption, Aerosol Sci. and Tech., 39, 40–51, doi: 10.1080/027868290901945, 2005.

Philpott, C.: Iron uptake in fungi: A system for every source, BBA-Mol Cell Res., 1763, 7, 636-645, 2006.

Philpott, C. C., Leidgens, S., and Frey, A. G.: Metabolic remodeling in iron-deficient fungi. Biochim Biophys Acta., 1823, 1509-1520, doi:10.1016/j.bbamcr.2012.01.012, 2012.

Prospero, J. M., Blades, E., Mathison, G. and Naidu, R.: Interhemispheric transport of viable fungi and bacteria from Africa to the Caribbean with soil dust, Aerobiologia, 21, 1-19, doi:10.1007/s10453-004-5872-7, 2005.

Prospero, J. M., Collard, F. X., Molinie, J. and Jeannot, A.: Characterizing the annual cycle of African dust transport to the Caribbean Basin and South America and its impact on air quality and the environment, Global Biogeochem. Cycles, 29, 757-773, doi:10.1002/2013GB004802, 2014.

Ravelo-Pérez, L. M., Rodríguez, S., Galindo, L., García, M. I., Alastuey, A. and López-Solano, J.: Soluble iron dust export in the high altitude Saharan Air Layer, Atmos. Env., 133:49-59, doi:10.1016/j.atmosenv.2016.03.030, 2016.

Remer, L. A., Kaufman, Y. J., Tandré, D., Mattoo, S., Chu, D. A., Martins, J. V., Li, R-R., Ichoku, C., Levy, R. C., Kleidman, R. G., Eck, T. F., Vermonte, E. and Holben, B. N.: The MODIS Aerosol Algorithm, Products, and Validation, Journal of the Atmospheric Sciences, Special Section Volume, 62, 947-973, doi:10.1175/JAS3385.1, 2005.

Reynolds, R. L., Cattle, S. R., Moskowitz, B. M., Goldstein, H. L., Yauk, K., Flagg, C. B., Berquó, T. S., Kokaly, R. F., Morman, S. and Breit, G. N.: Iron oxide minerals in dust of the Red Dawn event in eastern Australia, Aeolian Res., 15, 1-13, doi:10.1016/j.aeolia.2014.02.003, 2014.

Rienecker, M. R., Suarez, M. J., Gelaro, R., Todling, R., Bacmeister, J., Liu, E., Bosilovich, M. G., Schubert, S. D., Takacs, L., Kim, G. K., Bloom, S., Chen, J., Collins, D., Conaty, A., Silva, A., Gu, W., Joiner, J., Koster, R. D., Luchesi, R., Molod, A., Owens, T., Pawson, S., Pegion, P., Redder, C. R., Reichle, R., Robertson, F. R., Ruddick, A. G., Sienkiewich, M. and Woollen, J.: MERRA: NASA's Modern-Era Retrospective Analysis for Research and Applications, J. Climate, 24, 3624-3648, doi:10.1175/JCLI-D-11-00015.1, 2011.

Rizzo, L. V., Artaxo, P., Müller, T., Wiedensohler, A., Paixão, M., Cirino, G. G., Arana, A., Swietlicki, E., Roldin, P., Fors, E. O., Wiedemann, K. T., Leal, L. S. M. and Kulmala, M.: Long term measurements of aerosol optical properties at a primary forest site in Amazonia, Atmos. Chem. Phys., 13(17), 2391-2413, doi:10.5194/acp-13-2391, 2013.

Rizzo, L. V., Correia, A. L., Artaxo, P., Procópio, A. S. and Andreae, M. O.: Spectral dependence of aerosol light absorption over the Amazon Basin, Atmos. Chem. and Phys., 11, 8899–8912, doi: 10.5194/acp-11-8899-2011, 2011.

Roy, D. P., Boschetti, L., Justice, C. O. and Ju, J.: The Collection 5 MODIS Burned Area Product - Global Evaluation by Comparison with the MODIS Active Fire Product, Remote Sensing of Environ., 112, 3690-3707, 2008,

Salvador, P., Almeida, S. M., Cardoso, J., Almeida-Silva, M., Nunes, T., Cerqueira, M., Alves, C., Reis, M. A., Chaves, P. C., Artíñano, B. and Pio, C.: Composition and origin of PM10 in Cape Verde: characterization of long-range transport episodes, Atmos. Environ., 127, 326-339, doi:10.1016/j.atmosenv.2015.12.057, 2016.

Schepanski, K., Tegen, I. and Macke, A.: Comparison of satellite based observations of Saharan dust source areas, Remote Sens. Environ., 123, 90-97, doi:10.1016/j.rse.2012.03.019, 2012.

Schmink, M. and Wood, C.: Frontier Expansion in Amazonia, University of Florida press, Gainseville, Florida, 1978.

Schneider, C.A., Rasband, W.S. and Eliceiri, K.W.: NIH Image to ImageJ: 25 years of image analysis, Nature Methods, 9, 671-675, 2012.

Shi, Z., Bonneville, S., Krom, M. D., Carslaw, K. S., Jickells, T. D., Baker, A. R. and Benning, L. G.: Iron dissolution kinetics of mineral dust at low pH during simulated atmospheric processing, Atmos. Chem. Phys., 11, 995-1007, doi:10.5194/acp-11-995, 2011.

Siefert, R. L., Johansen A. M. and Hoffmann, M. R.: Measurements of trace metal (Fe, Cu, Mn, Cr) oxidation states in fog and stratus clouds, J. Air & Waste Manage. Assoc., 48, 128-143, doi:10.1080/10473289.1998.10463659, 1998.

Siefert, R. L.; Pehkonen, S. O.; Erel, Y. and Hoffmann, M. R.: Iron photochemistry of aqueous suspensions of ambient aerosol with added organic acids, Geochim. Cosmochim. Acta, 58 (15), 3271−3279, 1994.

Swap, R., Garstang, M., Greco, S. Talbot, R. and Kållberg, P.: Saharan dust in the Amazon Basin, Tellus, 44, 133-149, 1992.

Swap, R., Garstang, M., Macko, S., Tyson, P., Maenhaut, W., Artaxo, P., Kallberg, P. and Talbot, R.,: The long-range transport of southern African aerosols to the tropical South Atlantic, J. Geophy. Res., 101, 23777–23791, 1996.

Talbot, R. W., Andreae, M. O., Berresheim, H., Artaxo, P., Garstang, M., Harriss, R. C., Beecher, K. M. and Li, S. M.: Aerosol chemistry during the wet season in Central Amazonia: The influence of long-range transport, J. Geophys. Res., 95, 16,955-16,969, 1990.

Trail, F., Xu, H., Loranger. R. and Gadoury, D.: Physiological and environmental aspects of ascospore discharge in *Gibberella zeae* (anamorph *Fusarium graminearum*), Mycologia, 94, 181–189, 2002.

Trapp, J. M., Millero, F. J. and Prospero, J. M.: Trends in the solubility of iron in dust-dominated aerosols in the equatorial Atlantic trade winds: Importance of iron speciation and sources, Geochem. Geophys. Geosyst., 11, Q03014, doi:10.1029/2009GC002651, 2010.

~~U.S. Environmental protection Agency. Test Methods for Evaluating Soil Waste, Physical/Chemical Methods, Method 3052: Microwave assisted acid digestion of siliceous and organically based matrices. EPA SW-846, 1996.~~

U.S. Environmental ~~protection~~ Protection Agency. Determination of inorganic anions in drinking water by ion chromatography, Method 300.1. EPA, 1997.

Wang, Q., Saturno, J., Chi, X., Walter, D., Lavric, J. V., Moran-Zuloaga, D., Ditas, F., Pöhlker, C., Brito, J., Carbone, S., Artaxo, P., and Andreae, M. O., Modeling investigation of light-absorbing aerosols in the Amazon Basin during the wet season: Atmos. Chem. Phys., 16, 14,775-14,794, doi:10.5194/acp-16-14775-2016, 2016.

Washington, R. and Todd, M. C.: Atmospheric controls on mineral dust emission from the Bodélé Depression, Chad: The role of the low level jet, Geophys. Res. Lett., 32, L17701, doi:10.1029/2005GL023597, 2005.

Womack, A. M., Artaxo, P. E., Ishida, F. Y., Mueller, R. C., Saleska, S. R., Wiedemann, K. T., Bohannan, B. L. M. and Green, J. L.: Characterization of active and total fungal communities in the atmosphere over the Amazon rainforest, Biogeosciences, 12, 6337-6349, doi:10.5194/bg-12-6337, 2015.

Worobiec, A., Szalóki, I., Osán, J., Maenhaut, W., Stefaniak, E. A. and Grieken, R. V.: Characterization of Amazon Basin aerosols at the individual particle level by X-ray microanalytical techniques, Atmos. Environ., 41, 9217-9230, doi:10.1016/j.atmosenv.2007.07.056 , 2007.

Yamaguchi, N., Ichijo, T., Sakotani, A., Baba, T. and Nasu, M.: Global dispersion of bacterial cells on Asian dust, Sci. Rep., 2, 525, doi:10.1038/srep00525, 2012.

Yu, H., Chin, M., Yuan, T., Bian, H., Remer, L. A., Prospero, J. M., Omar, A., Winker, D., Yang, Y., Zhang, Y., Zhang, Z. and Zhao, C.: The fertilizing role of African dust in the Amazon rainforest: A first multiyear assessment based on data from Cloud-Aerosol Lidar and Infrared Pathfinder Satellite Observations, Geophys. Res. Lett., 42, 1984-1991, doi:10.1002/2015GL063040, 2015.

Zhang, Z., Engling, G., Zhang, L., Kawamura, K., Yang, Y., Tao, J., Zhang, R., Chan, C. and Li, Y.: Significant influence of fungi on coarse carbonaceous and potassium aerosols in a tropical rainforest, Environ. Res. Lett., 10, 034015, doi:10.1088/1748-9326/10/3/034015, 2015.

Zhu, X. R., Prospero, J. M. and Millero, F. J.: Diel variability of soluble Fe-(II) and soluble total Fe in North African dust in the trade winds at Barbados, J. Geophys. Res., 102, 21297-21305, doi:10.1029/97JD01313, 1997.

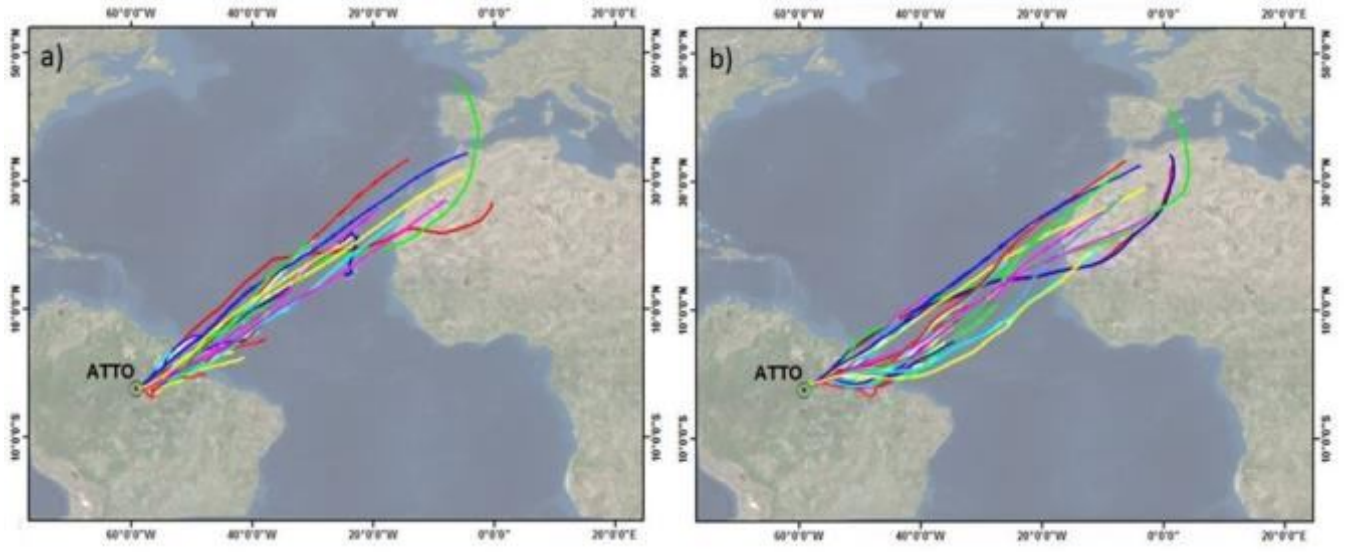

Figure 1. Backward trajectories of air parcels above the Amazon for 240 h during the sampling periods for: (a) 5 April 2015 and (b) 6 April 2015, when the greatest concentrations of dust from the Sahara arrived at ATTO.

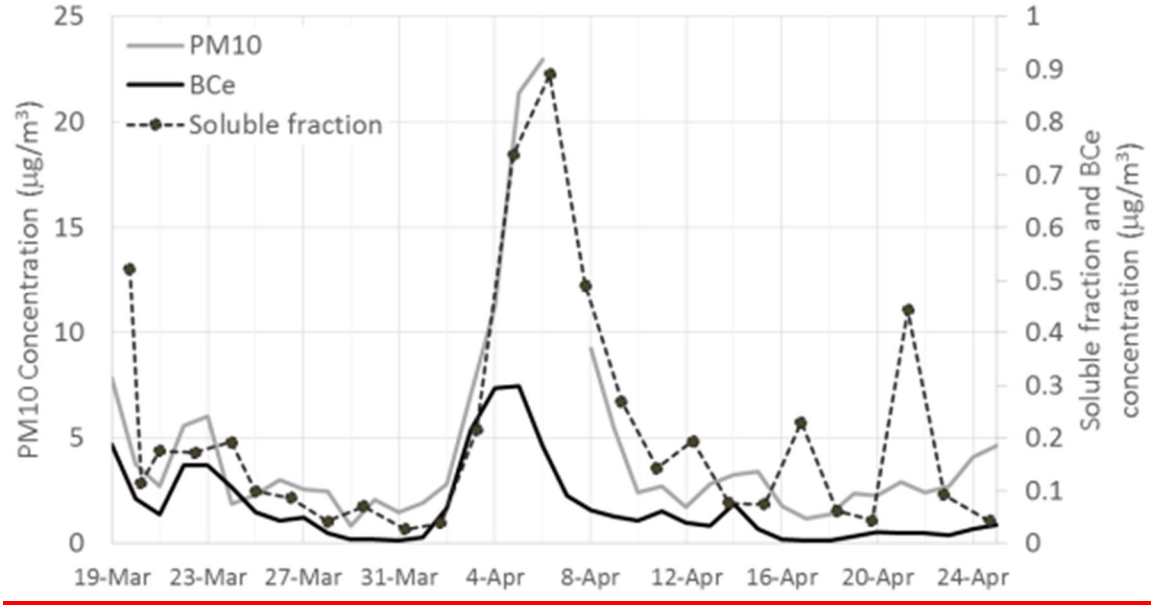

Figure 2. Time series of PM_{10} mass concentration, integrated from size distribution measurements (size range: 0.3-10 µm); black carbon equivalent (BCe) concentrations; and total concentration of particle soluble fraction.

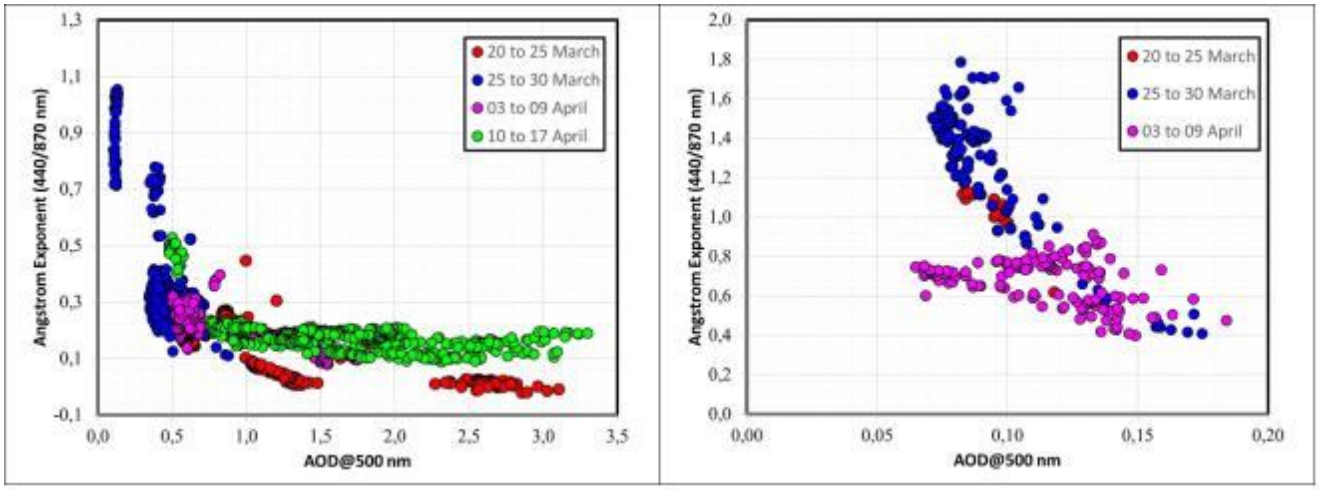

Figure 3. Ångström Exponent (AE) calculated using Aerosol Optical Depth (AOD) from 440 nm and 870 nm as a function of AOD at 500 nm (AOD@500 nm) using data from AERONET sunphotometers installed in Ilorin (08° 19' 12''N, 04° 20' 24''E - left plot) and upwind of Manaus in central Amazonia (02° 53' 12''S, 59° 58' 12''W - right plot) during distinct phases of the sampling period (20 March to 17 April).

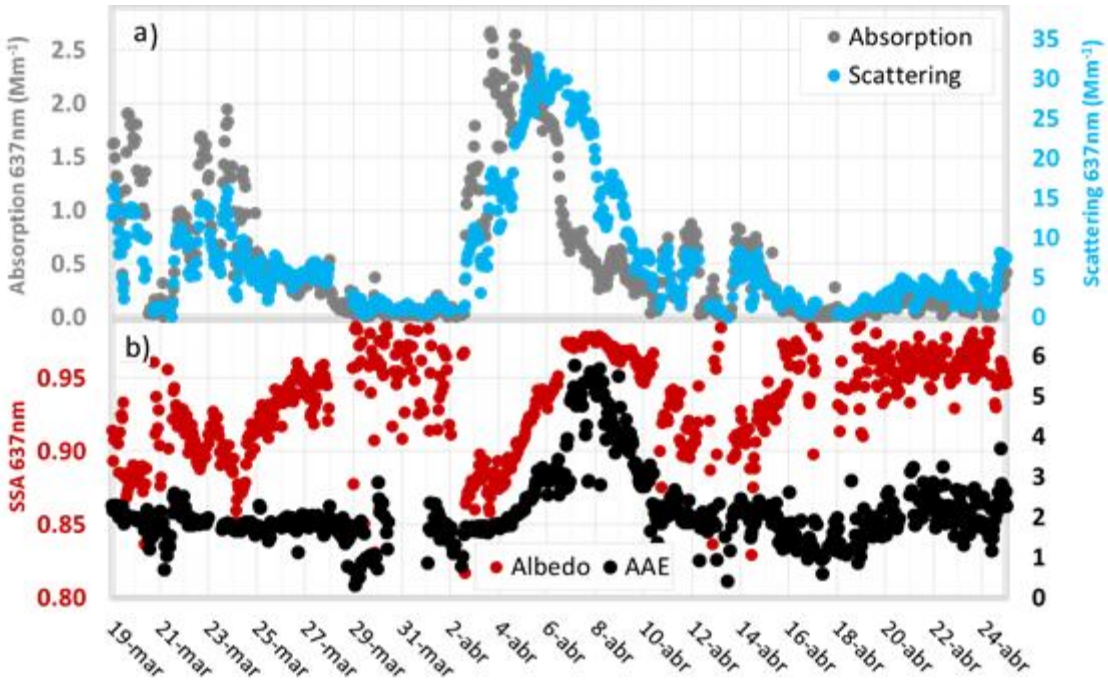

Figure 4. a) Particle absorption and scattering coefficients at 637 nm observed in situ at the ATTO site. b) Particle single scattering albedo (SSA) at 637 nm, and Absorption Ångström Exponent (AAE), retrieved from in situ observations of aerosol optical properties at ATTO.

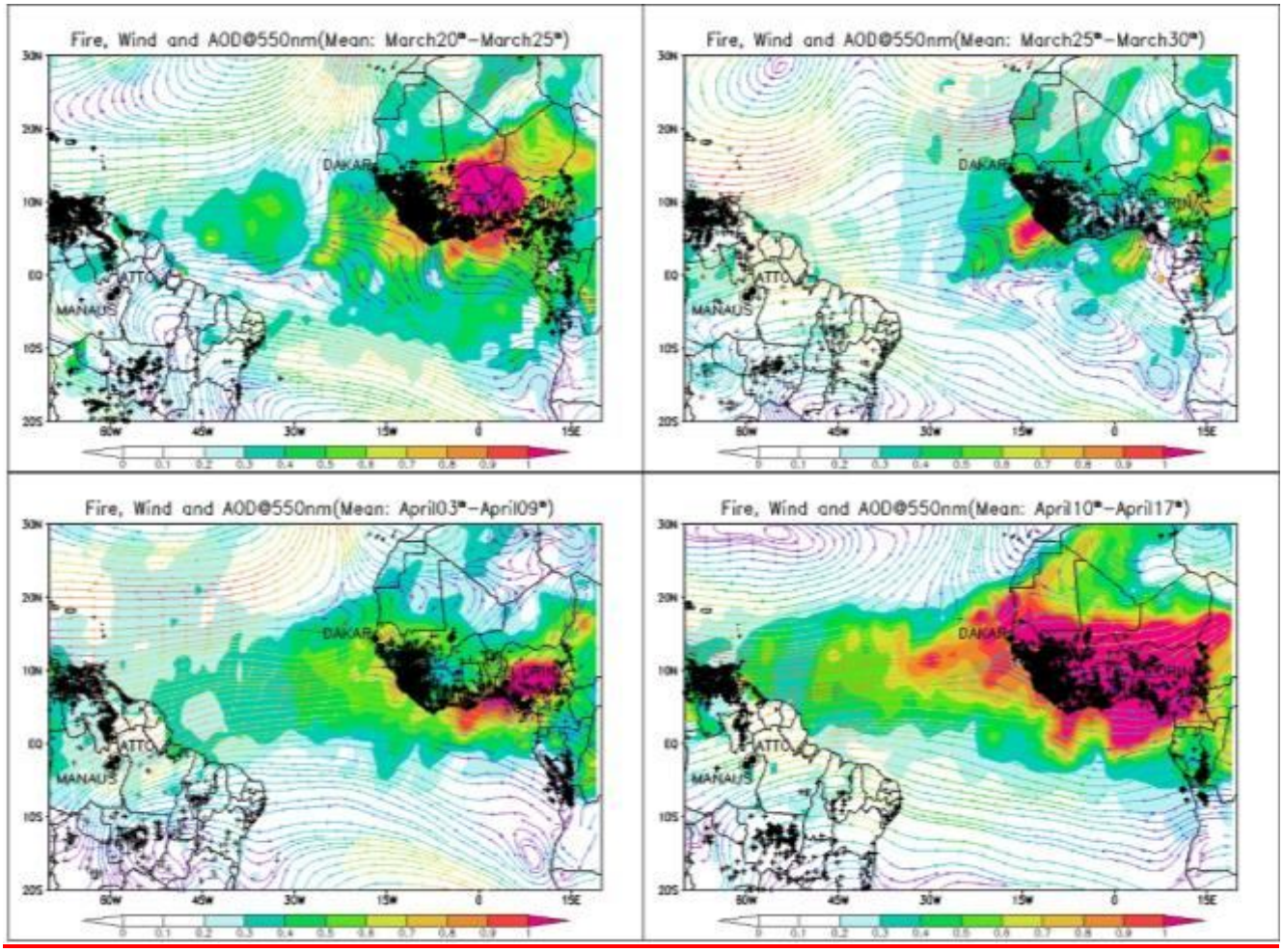

Figure 5. Mean aerosol optical depth at 550 nm (AOD, shaded colour) and wind at 850 hPa (stream lines) and total fire spots (black plus symbol) for four distinct periods within the campaign at ATTO site, during the dominance of: a) the first Saharan dust outbreak; b) a less active dust outbreak period; c) the second Saharan dust outbreak; d) the third Saharan dust outbreak.

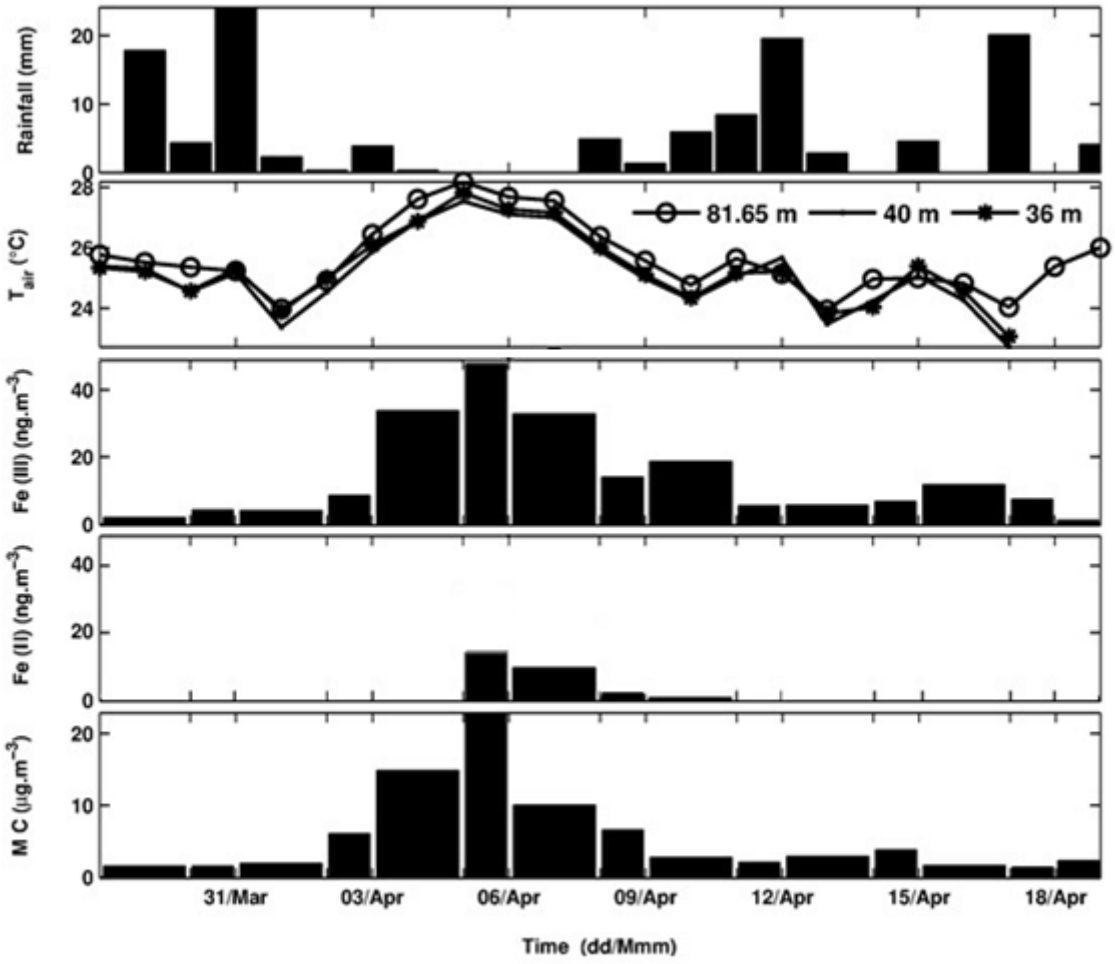

Figure 6. Daily comparison of micrometeorological variables: average air temperature and accumulated precipitation (Tair, Rainfall) with measurements of soluble Fe(III) and Fe(II) and mass concentration (MC) above the canopy.

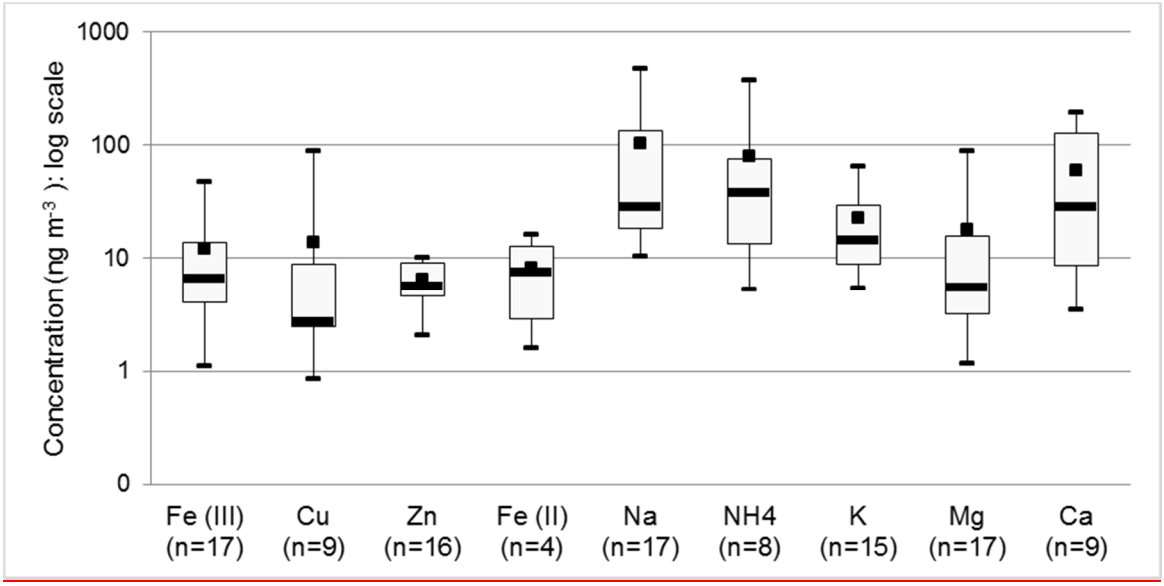

Figure 7. Boxplot for the soluble ion and other species concentrations in the total particulate matter samples at 60 m height from 30 March to 25 April 2015. Upper and lower whiskers represent 1.5 interquartile ranges for the period, upper and lower boundaries are for the third and first quartile. The horizontal bar is the median value and the black square is the average value for each element. In the horizontal axis the number of samples with valid results is shown.

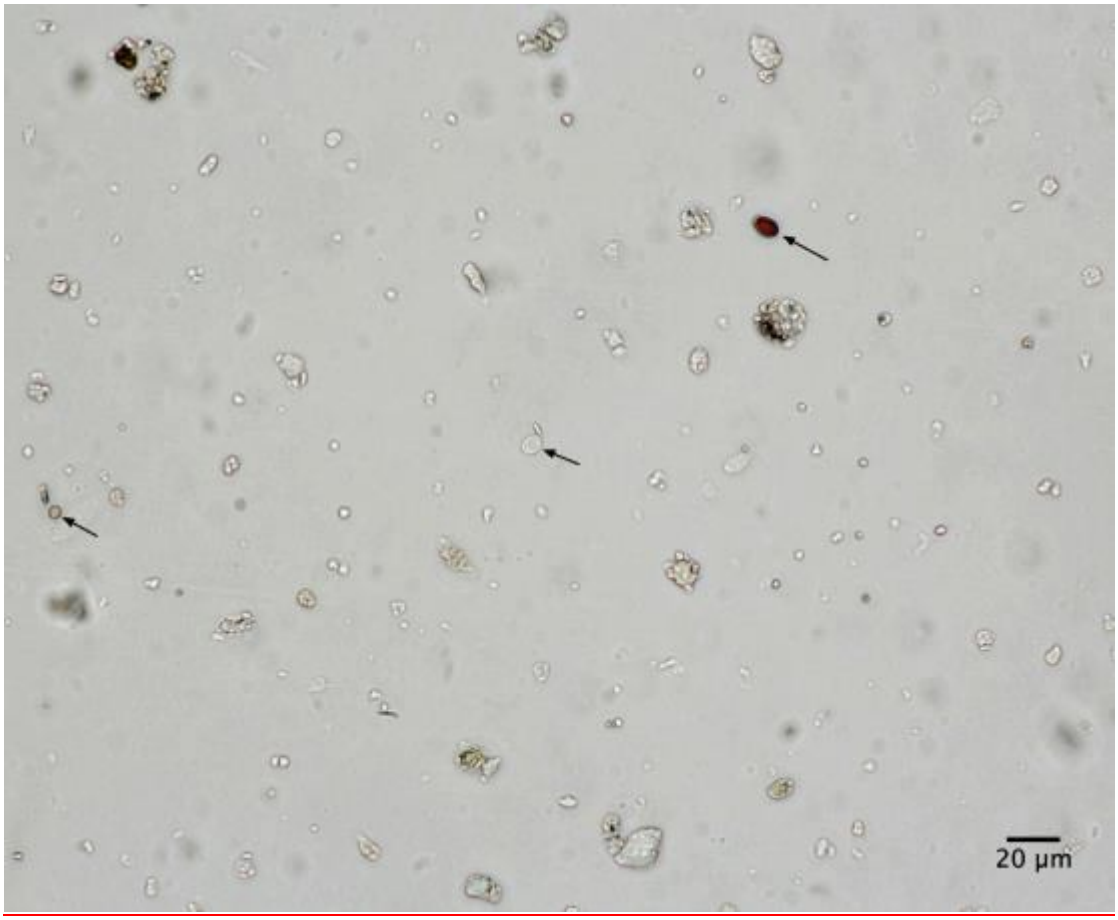

Figure 8. Brightfield microscope image of coarse particles and primary biological particles collected in the air sampler at ATTO at 80 m on 2 April 2015. The arrows point to three fungi: the one on the right is a coprinoid spore, at center is a yeast-like conidia, and at left is a small fungal spore of unknown type.